1978

Bearing Capacity of Surface Footings on a Sand Layer Resting on a Rigid Rough Base

Tom Walter Pfeifle

BEARING CAPACITY OF SURFACE FOOTINGS ON A SAND LAYER RESTING ON A RIGID ROUGH BASE

BY

TOM WALTER PFEIFLE

A thesis submitted
in partial fulfillment of the requirements for the
degree Master of Science, Major in
Engineering, South Dakota
State University

1978

BEARING CAPACITY OF SURFACE FOOTINGS ON A SAND LAYER RESTING ON A RIGID ROUGH BASE

This thesis is approved as a creditable and independent investigation by a candidate for the degree Master of Science, and is acceptable as meeting the thesis requirements for this degree, but without implying that the conclusions reached by the candidate are necessarily the conclusions of the major department.

Dr. Braja M. Das, Thesis Adviser — Date

Prof. Emory E. Johnson, Head
Civil Engineering Department — Date

ACKNOWLEDGMENTS

The writer is deeply indebted to his major adviser, Dr. Braja M. Das, Associate Professor of Civil Engineering, for the suggestion of this thesis topic and for his many long hours spent in encouraging and aiding the writer. Without his help, the completion of the writer's graduate studies would have been very difficult. In addition, the writer wishes to express his personal admiration for and friendship to Dr. Das.

Thanks go to Professor Emory E. Johnson, Civil Engineering Department Head, for providing the financial opportunity which made it possible for the writer to complete his graduate studies.

Thanks also go to Mr. T. Alvin Biggar, Technical Assistant, for his help in the construction of the writer's model test equipment.

A special note of thanks is due to the writer's wife, Mary, for her understanding and helpfulness during the many long hours required to complete this study.

TWP

TABLE OF CONTENTS

LIST OF TABLES

LIST OF ILLUSTRATIONS

NOTATIONS

$a = e^{(3/4\pi - \phi/2)\tan\phi}$

B = width of footing

$b = B/2$

c = cohesion of soil

C_a = cohesion force

C_u = coefficient of uniformity

D_1, D_2 = maximum depth from ground surface down to where the slip surfaces will extend

D_f = depth of footing below ground surface

G_s = specific gravity

H = depth of rigid base measured from the bottom of the foundation

K_{pc}, K_{pq}, $K_{p\gamma}$ = pure numbers whose values depend on the soil friction angle

L = length of footing

$m_1 = 1 - S'_q$

$m_2 = 1 - S'_\gamma$

N_c, N_q, N_γ = bearing capacity factors

N'_c, N'_q, N'_γ = modified bearing capacity factors

P_p = Rankine passive force

Q = vertical load applied to footing

q = uniform surcharge per unit area

q = load per unit area of the footing

q_u = ultimate load per unit area of the footing

r = radius at any point on a logarithmic spiral

r_o = initial radius on a logarithmic spiral

S = settlement

s = shear strength of soil

S'_q, S'_γ = shape factors

W = weight of soil wedge

δ = angle P_p makes with the normal line

γ = effective unit weight of soil

$\gamma d(max)$ = maximum dry density

$\gamma d(min)$ = minimum dry density

λ'_q, λ'_γ = modified shape factors

ϕ = internal angle of friction in soil

μ = angle sides of soil wedge makes with the horizontal

σ = normal stress

θ = angle between r_o and any other radial line

CHAPTER I

INTRODUCTION

In general engineering terms, 'foundation' refers to the lowest part of a structure. The function of a foundation is to transfer the load of a structure to the underlying soil on which it rests. Over-stressing of soil might result in excessive settlement and/or shear failure of soil. This stress condition may result in structural damage.

Depending upon the structure and the soil encountered, various types of foundations are used in practice. A 'spread footing' is simply an enlargement of a load bearing wall or column. This footing type makes it possible to spread the load of the structure over a large area of soil. Sometimes, due to low load-bearing capacity of soil, the size of spread footings becomes too large. In this case, it is economical to construct the entire structure over a concrete pad. This pad is referred to as a 'mat foundation'. 'Pile' and 'caisson' foundations are used for heavier structures where the depth required for supporting the soil is large.

Spread footings and mat foundations are generally referred to as shallow foundations. Pile and caisson foundations are classified as deep foundations. In order to give a quantitative definition, Terzaghi (1943), suggested that when the depth of a foundation is less than or equal to its width, it may be considered to be a shallow foundation.

This present study considers a shallow foundation which will later be referred to only as 'foundation'.

The ultimate bearing capacity of a shallow foundation is defined as the maximum unit pressure which can be supported at the base of a foundation. Beyond this unit pressure, shear failure in soil occurs.

In 1921, Prandtl published the results of his study for the penetration of hard bodies (metal punches) into another softer material from the viewpoint of plastic equilibrium. The softer material was assumed to be homogeneous and isotropic. This work of Prandtl was later extended by Terzaghi (1943) for the study of the ultimate soil bearing capacity for shallow foundations. Since that time, several investigators such as Meyerhof (1948, 1951), Caquot and Kerisel (1953), and Lundgren and Mortensen (1953), have refined the analysis proposed by Terzaghi. These theoretical developments have been supplemented by numerous small scale laboratory model studies and large scale field observations. All of these supplements have contributed to a better understanding of the load carrying capacity of shallow foundations.

In spite of the intensive investigations conducted by soils engineers around the world during the last 30 years or so, several aspects relating to the ultimate soil bearing capacity of shallow foundations yet remain to be studied. One of these aspects is the evaluation of the bearing capacity of foundations with a rigid base located at a rather shallow depth as measured from the bottom of the footing. In the Proceedings, Seventh International Conference on Soil Mechanics and Foundation Engineering (1969), Mandel and Salencon presented a

theoretical analysis for evaluating the ultimate soil bearing capacity for rough, shallow, strip foundations taking into consideration the effect of rigid bases located at shallow depths. Since then, however, a very limited amount of work (Meyerhof, 1974) has been done to verify the above mentioned theory.

The purpose of this study is to present the results of some recent laboratory model testing on the ultimate vertical load carrying capacity of rough, rectangular, surface footings which were placed on granular soil. A rigid base was located at limited depths. It is expected that these results will lend to a better quantitative understanding of the problem.

CHAPTER II

REVIEW OF PAST WORK

2.1. Terzaghi's Analysis of Soil Bearing Capacity for Shallow Strip Foundations

As pointed out in the introduction, most of the present refinements in the analysis of the ultimate soil bearing capacity for shallow foundations are based on the original study of Karl Terzaghi (1943). Terzaghi's original analysis may be explained through use of Fig. 2.1 in which a rough, strip footing of width, B, is located at a depth, D_f, below the ground surface. The ultimate load per unit area of the footing applied to cause soil failure is labeled as q_u. It is assumed that B is greater than or equal to D_f. The shear strength of the soil may be defined as (Fig. 2.2)

$$s = c + \sigma \tan \phi \tag{2.1}$$

where

s = shear strength of soil,

c = cohesion,

σ = normal stress,

and

ϕ = angle of friction

For shallow foundations, Terzaghi assumed that the soil above the bottom of the footing may be replaced by a uniform surcharge of $q = \gamma D_f$.

When the ultimate load, q_u, is applied to the footing, shear failure in soil will occur. The boundaries of the zones of plastic

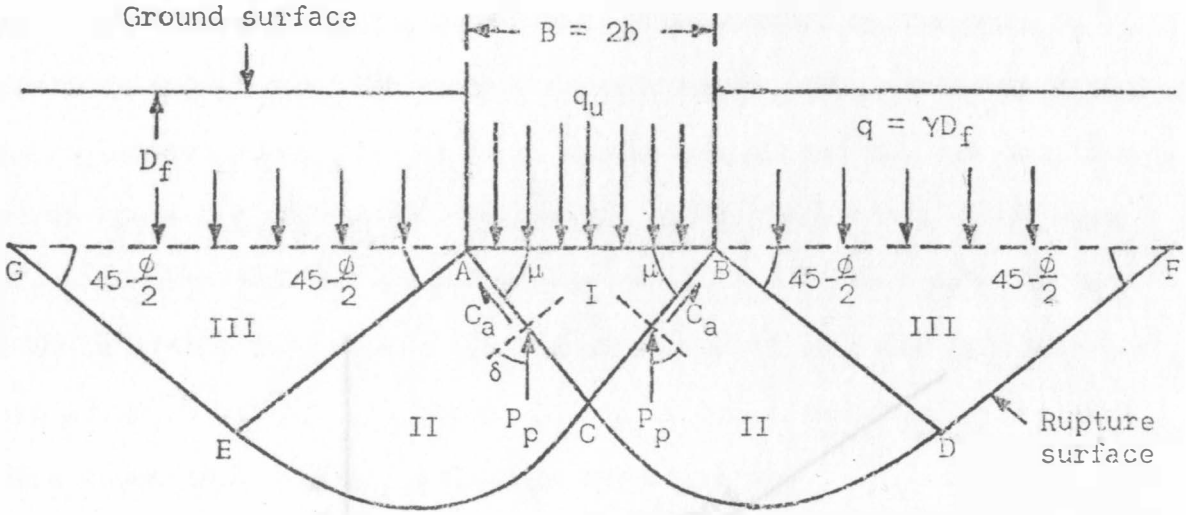

(a)

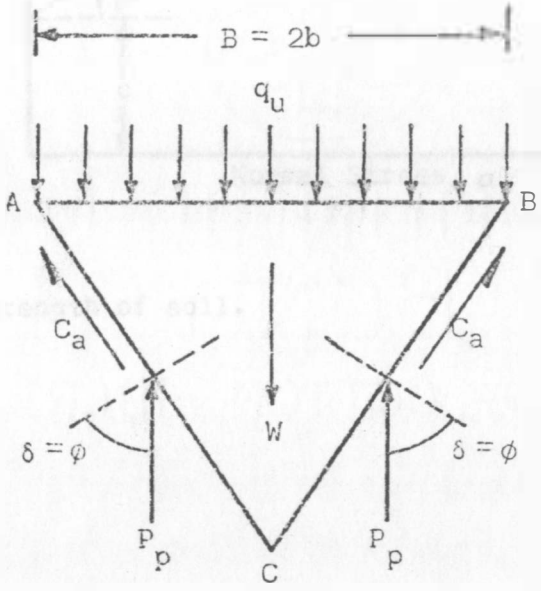

(b)

Fig. 2.1. Terzaghi's soil bearing capacity analysis for rough, strip footings.

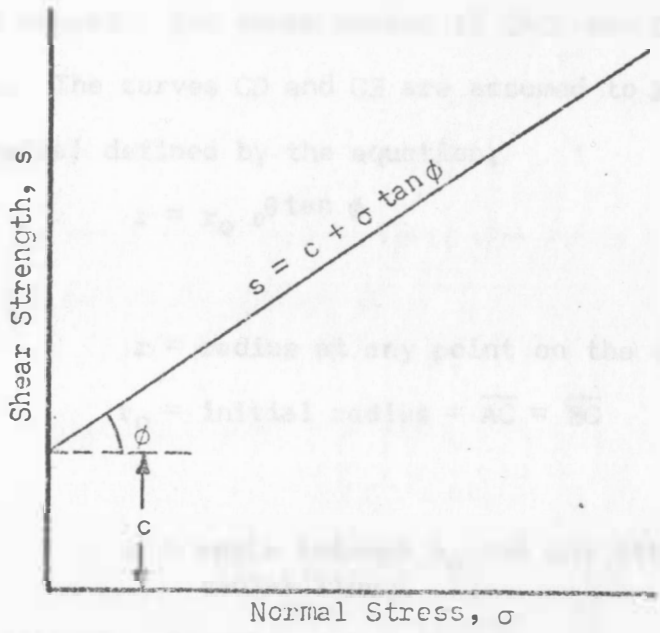

Fig. 2.2. Shear strength of soil.

flow after failure of the earth support as assumed by Terzaghi is shown in Fig. 2.1a. The triangular soil wedge, ABC, marked as Zone I is an elastic zone. The sides of the wedge, AC and BC, are inclined at an angle $\mu = \phi$ with the horizontal. At failure, this wedge moves downward with the footing and pushes the soil mass in areas BCDF and ACEG laterally and upward. The zones marked II (ACE and BCD) are the radial shear zones. The curves CD and CE are assumed to be the arcs of a logarithmic spiral defined by the equation,

$$r = r_o \, e^{\theta \tan \phi} \tag{2.2}$$

where

r = radius at any point on the curve,

r_o = initial radius = $\overline{AC} = \overline{BC}$

and

θ = angle between r_o and any other radial line

The zones marked III (AEG and BDF) are Rankine passive zones. The rupture surfaces, DF and EG, are straight lines. The lines BD, DF, AE, and EG make angles of $45 - \frac{\phi}{2}$ with the horizontal.

At failure, the passive force, P_p, will act along each face of the soil wedge, ABC. Since the soil friction angle is equal to ϕ, the line of action of P_p will be inclined at an angle, ϕ, to the normal line drawn to the wedge faces. This means that the direction of P_p is vertically upward.

The ultimate bearing capacity can now be analyzed by considering the free body diagram of the wedge, ABC (Fig. 2.1b). Considering a unit length of the footing for vertical equilibrium,

$$(q_u)\,(2b)\,(1) = -W + 2C_a \sin\phi + 2P_p \tag{2.3}$$

where

$b = B/2$,

W = weight of the soil wedge, ABC, $= \gamma b^2 \tan\phi$,

and

C_a = cohesive force acting along the faces,

AC and BC, $= c(b/\cos\phi)$.

Thus,

$$2bq_u = 2P_p + 2bc\tan\phi - \gamma b^2 \tan\phi \tag{2.4}$$

In the above equation, P_p may be expressed as

$$P_p = b/\cos^2\phi\left[cK_{pc} + qK_{pq}\right] + \frac{\gamma b^2}{2}\frac{\tan\phi}{\cos^2\phi}\,K_{p\gamma} \tag{2.5}$$

where K_{pc}, K_{pq}, and $K_{p\gamma}$ are pure numbers whose values depend on the angle of soil friction, ϕ.

Substitution of Eq. 2.5 into 2.4 yields,

$$q_u = \underbrace{\tfrac{1}{2}\gamma B\left[\tfrac{1}{2}\tan\phi\left(\frac{K_{p\gamma}}{\cos^2\phi} - 1\right)\right]}_{N_\gamma} + c\underbrace{\left[\frac{K_{pc}}{\cos^2\phi} + \tan\phi\right]}_{N_c} + q\underbrace{\left[\frac{K_{pq}}{\cos^2\phi}\right]}_{N_q}$$

or

$$q_u = cN_c + qN_q + \tfrac{1}{2}\gamma BN_\gamma \tag{2.6}$$

The terms N_c, N_q, and N_γ in the above equation are known as bearing capacity factors. The solution to these factors are extremely tedious and time consuming. For this reason, Terzaghi used an approximate method of superposition to determine these factors. The method of superposition may be defined as follows:

(1) For a weightless soil (i.e., $\gamma = 0$), if $q = 0$ (i.e., surface footing), then

$$q_u = cN_c \tag{2.7}$$

Solution for this condition yields,

$$N_c = \cot\phi\left[\frac{a^2}{2\cos^2\left(45 + \frac{\phi}{2}\right)} - 1\right] \tag{2.8}$$

where $a = e^{\left(\frac{3}{4}\pi - \frac{\phi}{2}\right)\tan\phi}$ (2.9)

(2) For a weightless soil (i.e., $\gamma = 0$), if $c = 0$, then

$$q_u = qN_q \tag{2.10}$$

Solution of this condition gives,

$$N_q = \frac{a^2}{2\cos^2\left(45 + \frac{\phi}{2}\right)} \tag{2.11}$$

where 'a' is given by Eq. 2.9.

(3) For a surface footing in cohesionless soil, (i.e., $q = 0$, $c = 0$, and $\gamma \neq 0$),

$$q_u = \tfrac{1}{2}\gamma BN_\gamma \tag{2.12}$$

$$\text{where } N_\gamma = \tfrac{1}{2}\tan\phi\left(\frac{K_{p\gamma}}{\cos^2\phi} - 1\right) \qquad (2.13)$$

The values of $K_{p\gamma}$ for various angles of soil friction, ϕ, obtained by Terzaghi are given in Table 2.1.

The method of superposition described above is not an exact solution. However, it yields an estimation which is on the safe side for evaluating the ultimate bearing capacity of shallow, strip foundations (Terzaghi, 1943).

TABLE 2.1

VALUE OF $K_{p\gamma}$ (Eq. 2.13)

ϕ (deg.)	$K_{p\gamma}$
0	10.8
5	12.2
10	14.4
15	18.6
20	25.0
25	35.0
30	52.0
35	82.0
40	141.0
45	298.0

2.2. Modifications to Terzaghi's General Bearing Capacity Equation

At the time of the development of Terzaghi's bearing capacity analysis, a very limited amount of experimental results was available. Extensive laboratory and field tests since then show that the basic assumption of the failure mechanism adopted by Terzaghi (Fig. 2.1a) was essentially correct. However, the angle μ, which the sides AC and BC of the triangular wedge, ABC, make with the horizontal, is about $45 + \frac{\phi}{2}$ instead of ϕ (for example: DeBeer and Vesić, 1958).

With the assumption of $\mu = 45 + \frac{\phi}{2}$, the bearing capacity factors, N_c, N_q, and N_γ, will be somewhat changed. The ultimate soil bearing capacity of shallow, strip footings can still be expressed in the same form as Eq. 2.6. That is,

$$q_u = cN_c + qN_q + \tfrac{1}{2}\gamma BN_\gamma$$

Using Terzaghi's method of superposition for a surface footing ($q = 0$) on a weightless soil ($\gamma = 0$), the ultimate soil bearing capacity can be expressed by

$$q_u = cN_c$$

Prandtl (1921) has given the value of N_c as

$$N_c = \left[e^{\pi \tan \phi} \tan^2 \left(\frac{\pi}{4} + \frac{\phi}{2}\right) - 1 \right] \cot \phi \qquad (2.14)$$

A comparison of the values of N_c obtained from Terzaghi's solution (Eq. 2.8) with those obtained by Prandtl (Eq. 2.14) is shown in Fig. 2.3. For the range of $\phi = 0^\circ$ to 45°, Prandtl's values are seen to be from 10 to 23 percent lower than those presented by Terzaghi.

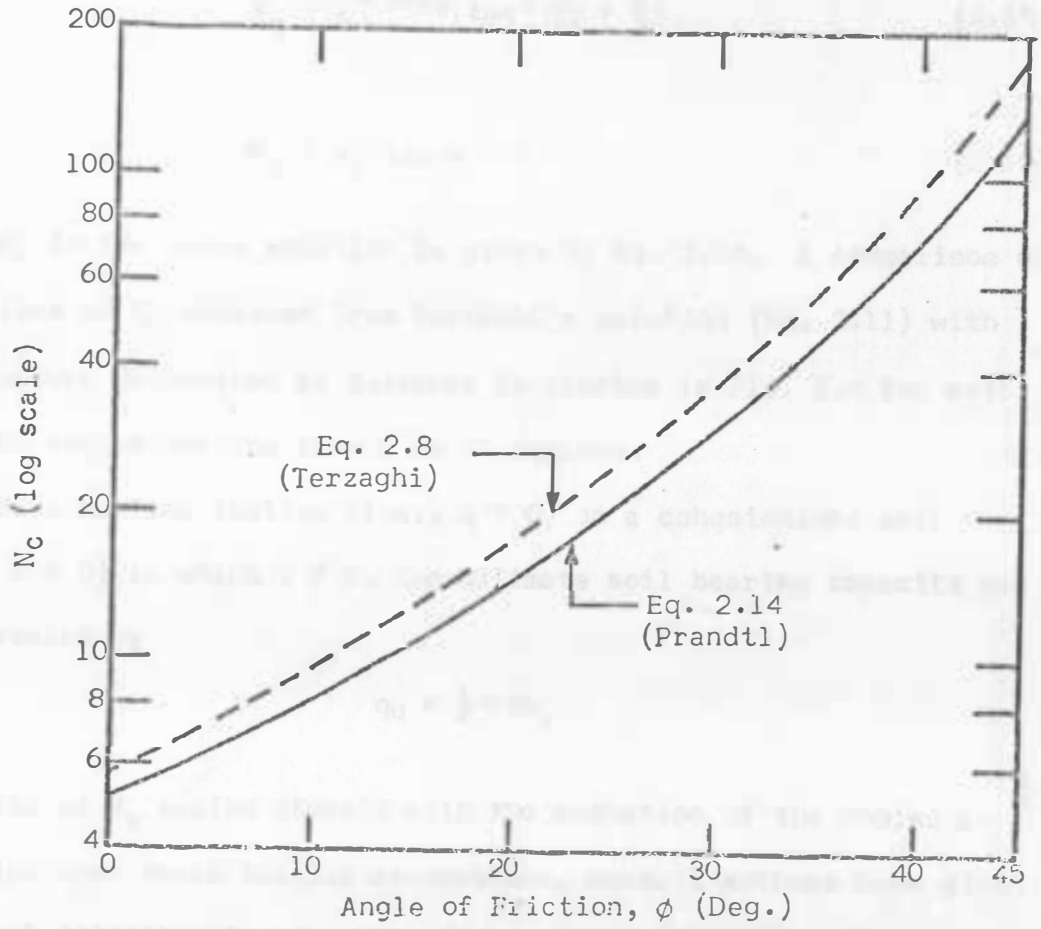

Fig. 2.3. Comparison between Terzaghi's and Prandtl's values of N_c.

Again, for a weightless soil (i.e., $\gamma = 0$), if $c = 0$, then

$$q_u = qN_q$$

For such a case, Reissner (1924) has derived the value of N_q. It can be given by

$$N_q = e^{\pi \tan\phi} \tan^2 \left(\frac{\pi}{4} + \frac{\phi}{2}\right) \tag{2.15}$$

or

$$N_q = N_c \tan \phi + 1 \tag{2.16}$$

where N_c in the above equation is given by Eq. 2.14. A comparison of the values of N_q obtained from Terzaghi's solution (Eq. 2.11) with those values determined by Reissner is plotted in Fig. 2.4 for soil friction angles varying from 0 to 45 degrees.

For a surface footing (i.e., $q = 0$) on a cohesionless soil (i.e., $c = 0$) in which $\gamma \neq 0$, the ultimate soil bearing capacity can be expressed by

$$q_u = \tfrac{1}{2} \gamma B N_\gamma$$

The value of N_γ varies sharply with the variation of the angle, μ. Depending upon their initial assumptions, several authors have given numerical solutions for N_γ. Caquot and Kerisel (1953) used Boussinesq's original differential equations which considered the weight of the material. Assuming $\mu = 45 + \frac{\phi}{2}$ and using a method of successive approximation, they presented a set of N_γ values for various soil friction angles, ϕ. Vesić (1973) has suggested that with small errors (not exceeding 10 percent for $15^\circ < \phi < 45^\circ$ and not exceeding

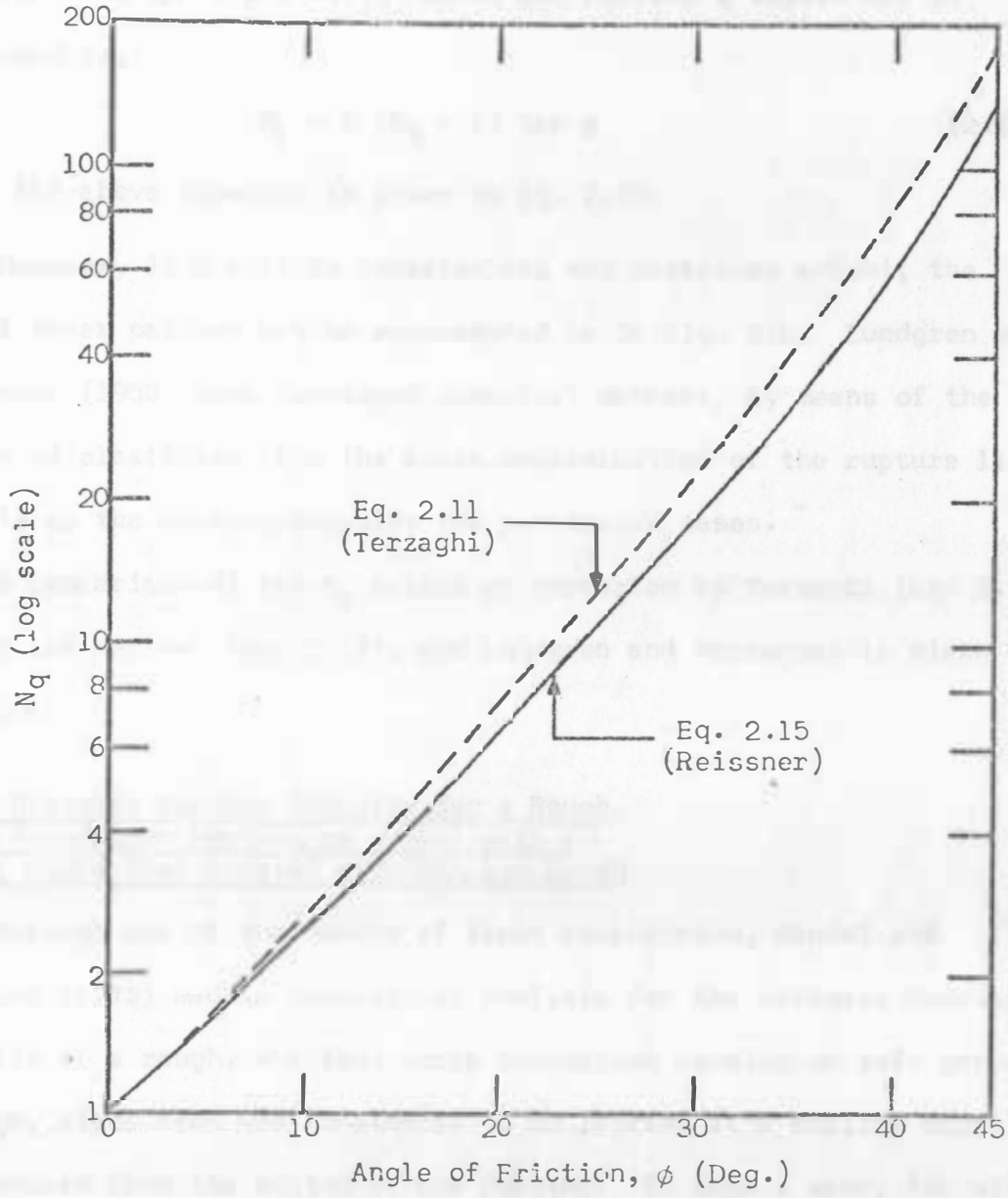

Fig. 2.4. Comparison between Terzaghi's and Reissner's values of N_q.

5 percent for $20^{\circ} < \phi < 40^{\circ}$), Caquot and Kerisel's values may be expressed as,

$$N_{\gamma} = 2 (N_q + 1) \tan \phi \qquad (2.17)$$

N_q in the above equation is given by Eq. 2.15.

However, if a soil is cohesionless and possesses weight, the actual shear pattern may be represented as in Fig. 2.5. Lundgren and Mortensen (1953) have developed numerical methods, by means of the theory of plasticity, for the exact determination of the rupture lines as well as the bearing capacity for particular cases.

A comparison of the N_{γ} values as presented by Terzaghi (Eq. 2.13), Caquot and Kerisel (Eq. 2.17), and Lundgren and Mortensen is given in Fig. 2.6.

2.3. Ultimate Bearing Capacity for a Rough, Strip Foundation Resting on a Soil with a Rough, Rigid Base Located at a Shallow Depth

Through use of the theory of limit equilibrium, Mandel and Salencon (1972) made a theoretical analysis for the ultimate bearing capacity of a rough, shallow, strip foundation resting on soft ground. A rough, rigid base was considered to be located at a shallow depth as measured from the bottom of the footing. In such a case, the ultimate bearing capacity may be expressed in a form similar to Eq. 2.6. That is,

$$q_u = cN'_c + qN'_q + \tfrac{1}{2}\gamma BN'_{\gamma} \qquad (2.18)$$

where N'_c, N'_q, and N'_{γ} are the modified bearing capacity factors and $q = \gamma D_f$. In evaluating the modified bearing capacity factors, Mandel

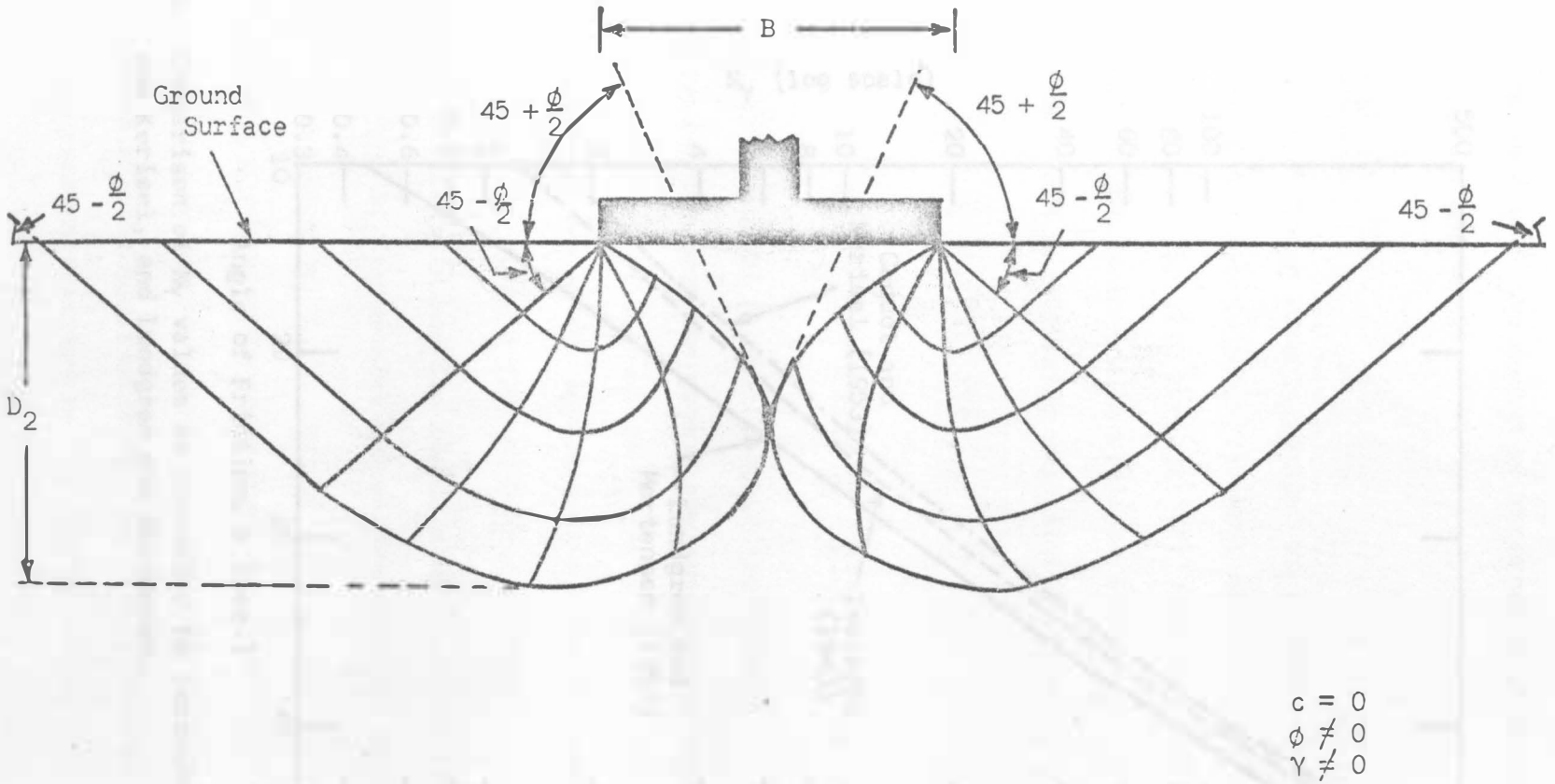

Fig. 2.5. Shear pattern in soil for a rough surface footing ($c = 0$, $\phi \neq 0$, $\gamma \neq 0$).

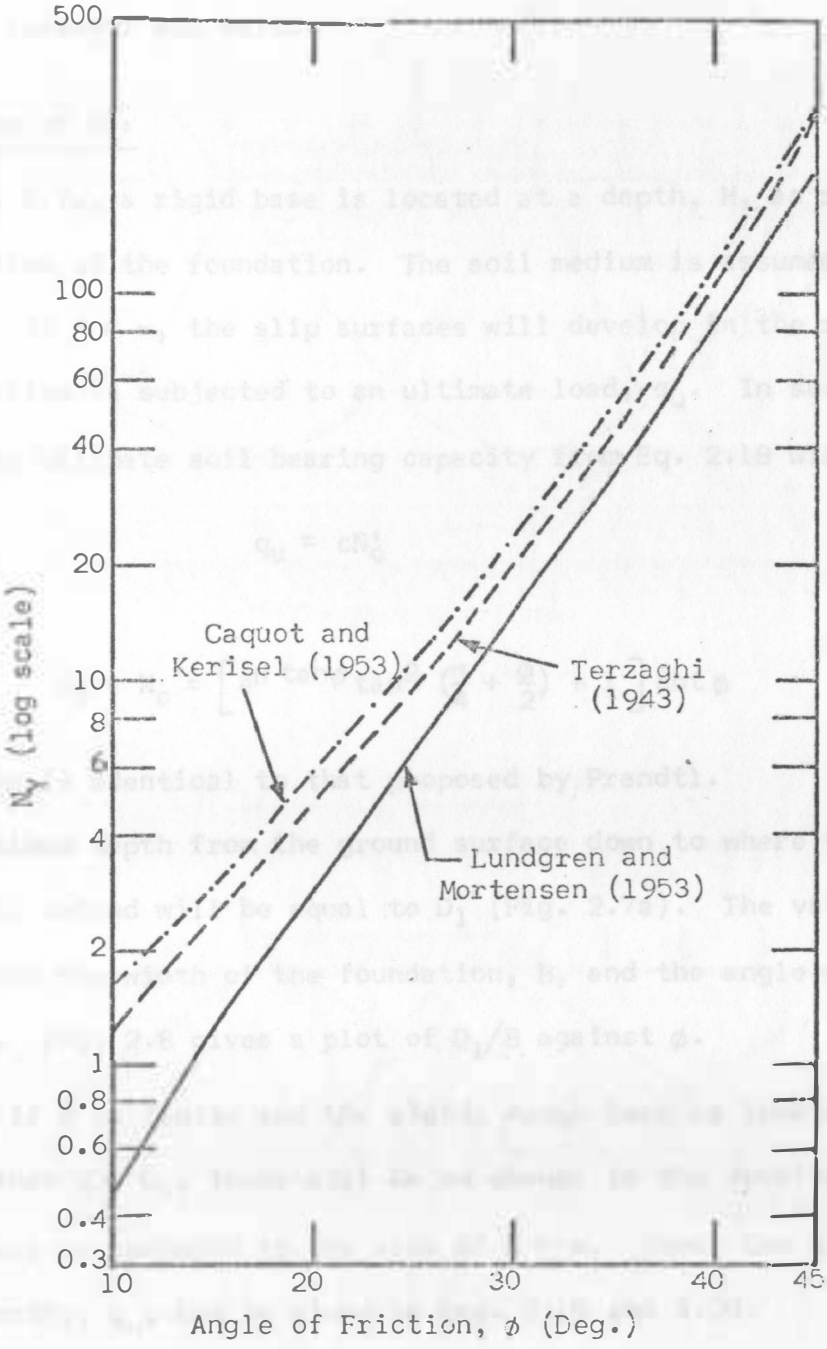

Fig. 2.6. Comparison of N_γ values as presented by Terzaghi, Caquot and Kerisel, and Lundgren and Mortensen.

and Salencon assumed that the method of superposition originally introduced by Terzaghi was valid.

Determination of N'_c:

In Fig. 2.7a, a rigid base is located at a depth, H, as measured from the bottom of the foundation. The soil medium is assumed to be weightless. If $H = \infty$, the slip surfaces will develop in the soil mass when the footing is subjected to an ultimate load, q_u. In such a case, if $q = 0$, the ultimate soil bearing capacity from Eq. 2.18 will be

$$q_u = cN'_c \tag{2.19}$$

where

$$N'_c = N_c = \left[e^{\pi \tan\phi} \tan^2 \left(\frac{\pi}{4} + \frac{\phi}{2}\right) - 1 \right] \cot\phi \tag{2.20}$$

This solution is identical to that proposed by Prandtl.

The maximum depth from the ground surface down to where the slip surfaces will extend will be equal to D_1 (Fig. 2.7a). The value of D_1 will depend on the width of the foundation, B, and the angle of soil friction, ϕ. Fig. 2.8 gives a plot of D_1/B against ϕ.

Again, if H is finite and the rigid, rough base is located at a depth such that $H \geq D_1$, there will be no change in the development of the slip lines as compared to the case of $H = \infty$. Thus, the ultimate bearing capacity, q_u, can be given by Eqs. 2.19 and 2.20.

If however $H < D_1$, the development of the slip lines at failure will be modified as shown in Fig. 2.7b. In that case, the soil mass in the zone cde remains motionless. The rigid wedge, abc, sinks

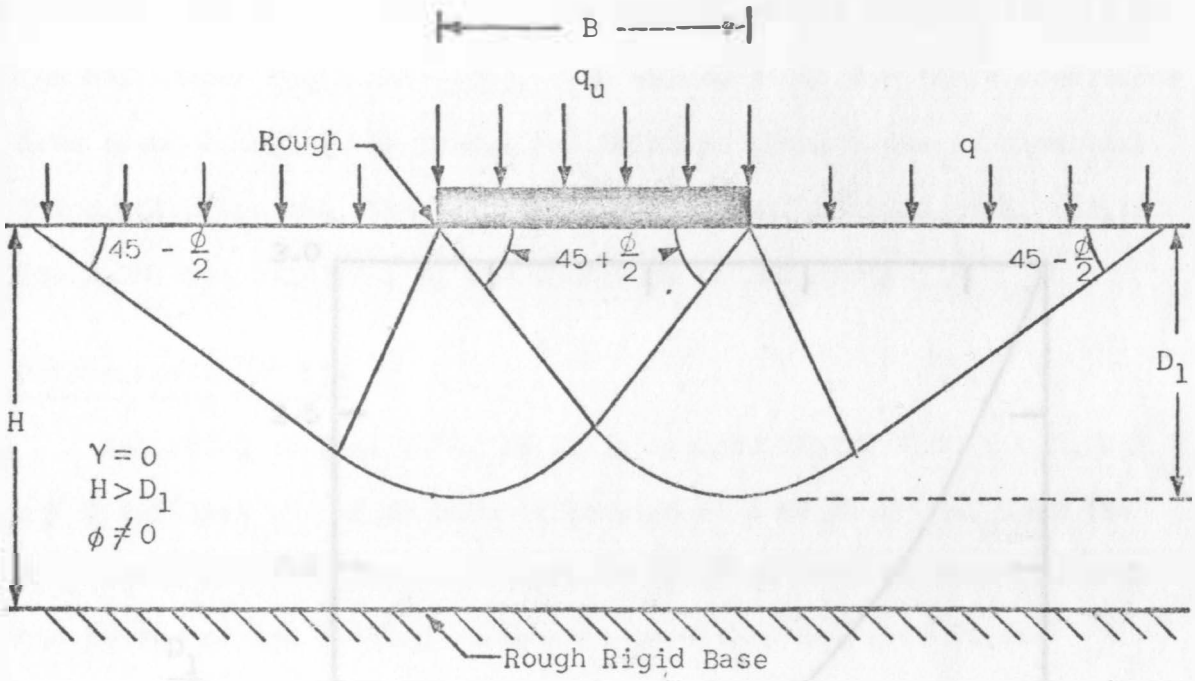

(a)

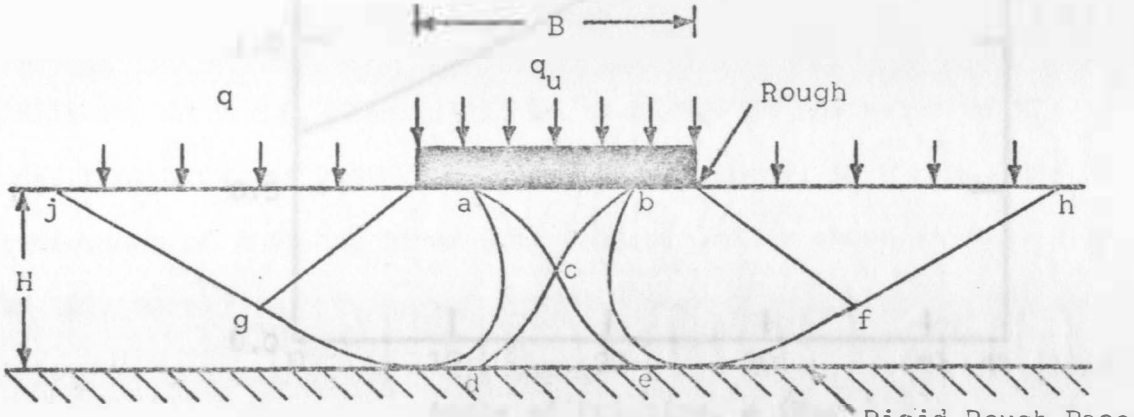

(b)

Fig. 2.7. Effect of a rigid base on the slip surface in soil ($\gamma = 0$, $\phi \neq 0$) for bearing capacity failures.

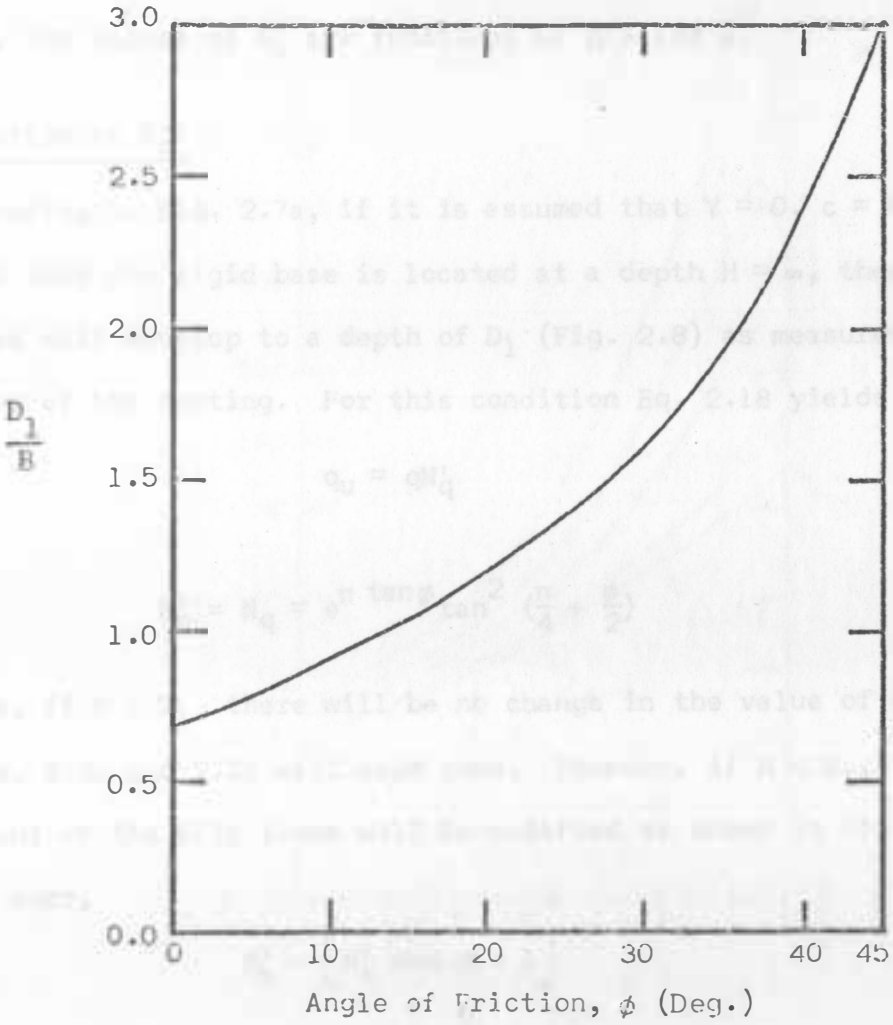

Fig. 2.8. Plot of D_1/B against ϕ (after Mandel and Salencon).

downward with the foundation. This sinking causes plastic failure in the soil zones bcefh and acdgj. The values of N'_c for these conditions have been determined by Mandel and Salencon through use of numerical integration and are given in Fig. 2.9. It may be noted that, unlike Eq. 2.20, the values of N'_c are functions of H/B and ϕ.

Determination of N'_q:

Referring to Fig. 2.7a, if it is assumed that $\gamma = 0$, $c = 0$, but $q \neq 0$ and that the rigid base is located at a depth $H = \infty$, then the slip lines will develop to a depth of D_1 (Fig. 2.8) as measured from the bottom of the footing. For this condition Eq. 2.18 yields

$$q_u = qN'_q \tag{2.21}$$

where

$$N'_q = N_q = e^{\pi \tan\phi} \tan^2 \left(\frac{\pi}{4} + \frac{\phi}{2}\right) \tag{2.22}$$

Similarly, if $H \geq D_1$, there will be no change in the value of N'_q. Thus, Eqs. 2.21 and 2.22 will hold good. However, if $H < D_1$, the development of the slip lines will be modified as shown in Fig. 2.7b. For this case,

$$N'_q = \left[N'_c \tan \phi + 1\right] \tag{2.23}$$

where N'_c is a bearing capacity factor given in Fig. 2.9.

Fig. 2.10 gives the plot of N'_c for various values of D_1/B and ϕ.

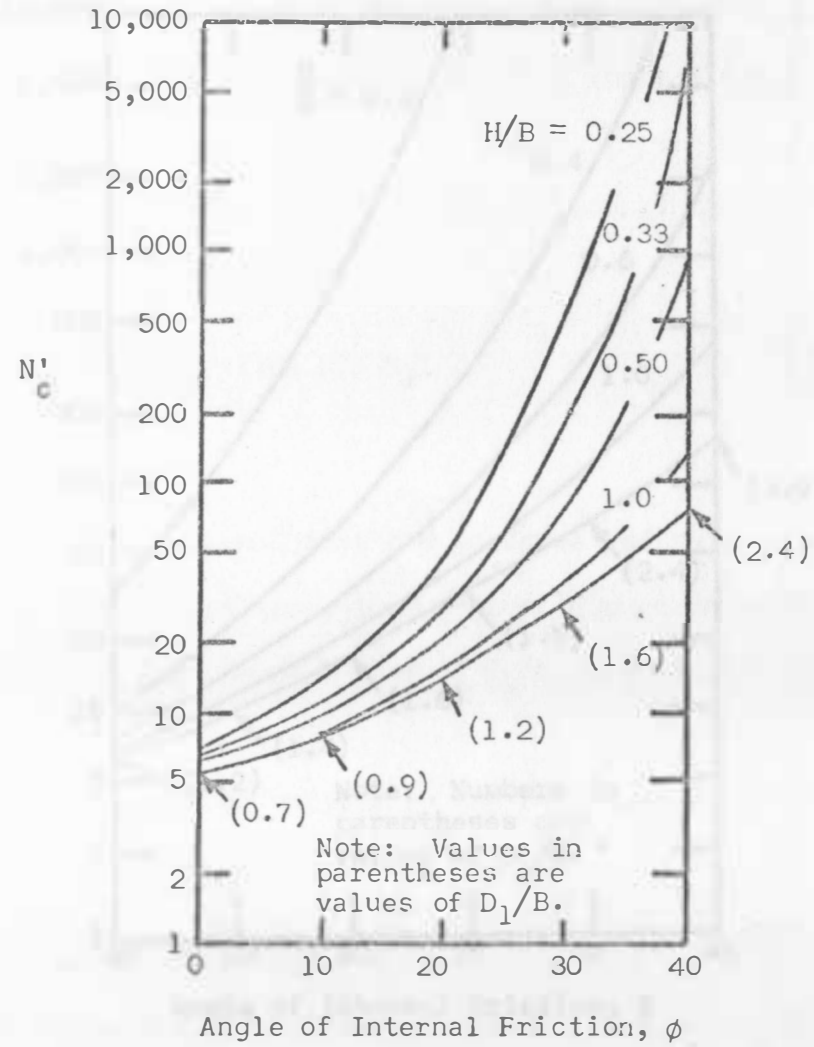

Fig. 2.9. Plot of N'_c against ϕ (after Mandel and Salencon, 1972).

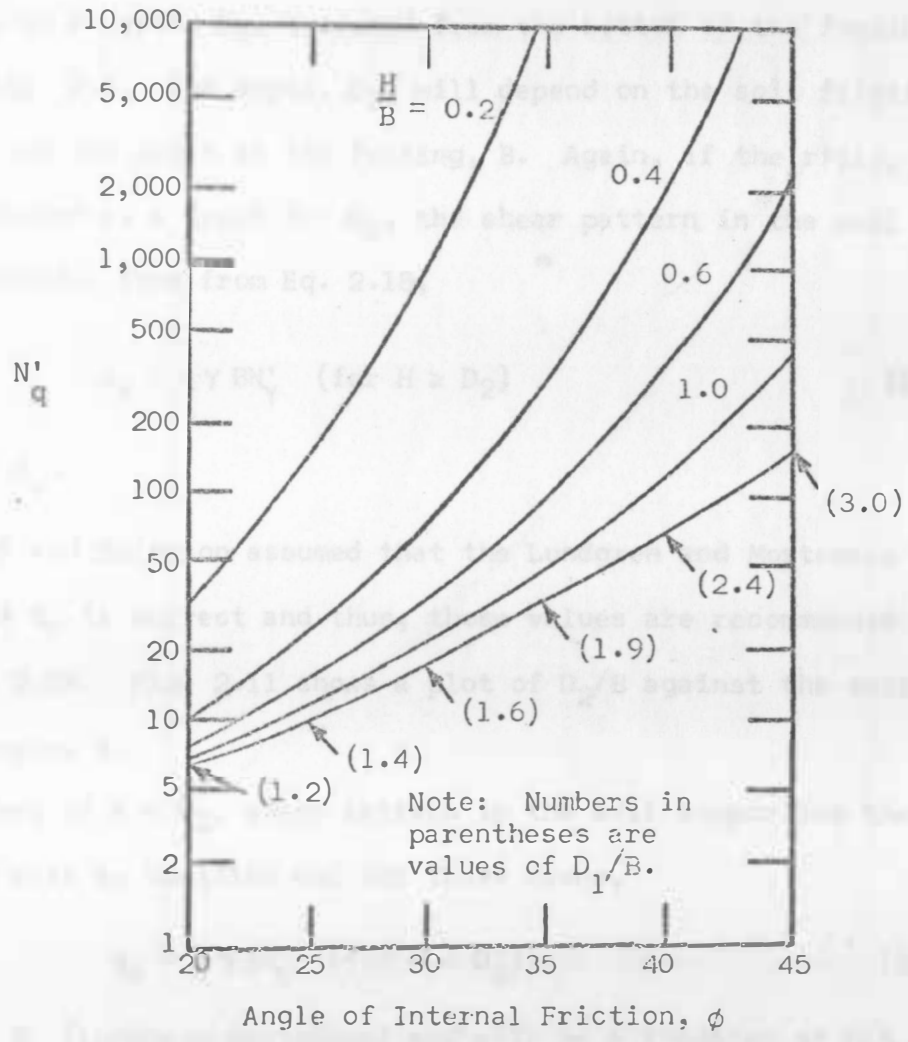

Fig. 2.10. Plot of N'_q against ϕ (after Meyerhof, 1974, from the numerical values of Mandel and Salencon).

Determination of N'_γ:

For a surface footing on a cohesionless soil (i.e., c = 0 and q = 0), if $\gamma \neq 0$ and $H = \infty$, the slip lines at ultimate load will develop up to a depth, D_2, measured from the bottom of the footing as shown in Fig. 2.5. The depth, D_2, will depend on the soil friction angle, ϕ, and the width of the footing, B. Again, if the rigid, rough base is located at a depth $H = D_2$, the shear pattern in the soil will not be changed. Thus from Eq. 2.18,

$$q_u = \tfrac{1}{2}\gamma B N'_\gamma \quad (\text{for } H \geq D_2) \tag{2.24}$$

where $N'_\gamma = N_\gamma$.

Mandel and Salencon assumed that the Lundgren and Mortensen type solution of N_γ is correct and thus, those values are recommended for use in Eq. 2.24. Fig. 2.11 shows a plot of D_2/B against the soil friction angle, ϕ.

However, if $H < D_2$, shear pattern in the soil supporting the foundation will be modified and for those cases,

$$q_u = \tfrac{1}{2}\gamma B N'_\gamma \quad (\text{for } H < D_2) \tag{2.25}$$

where $N'_\gamma > N_\gamma$ (Lundgren-Mortensen) and will be a function of H/B and ϕ.

Fig. 2.12 gives the variation N'_γ with the soil friction angle, ϕ, and H/B.

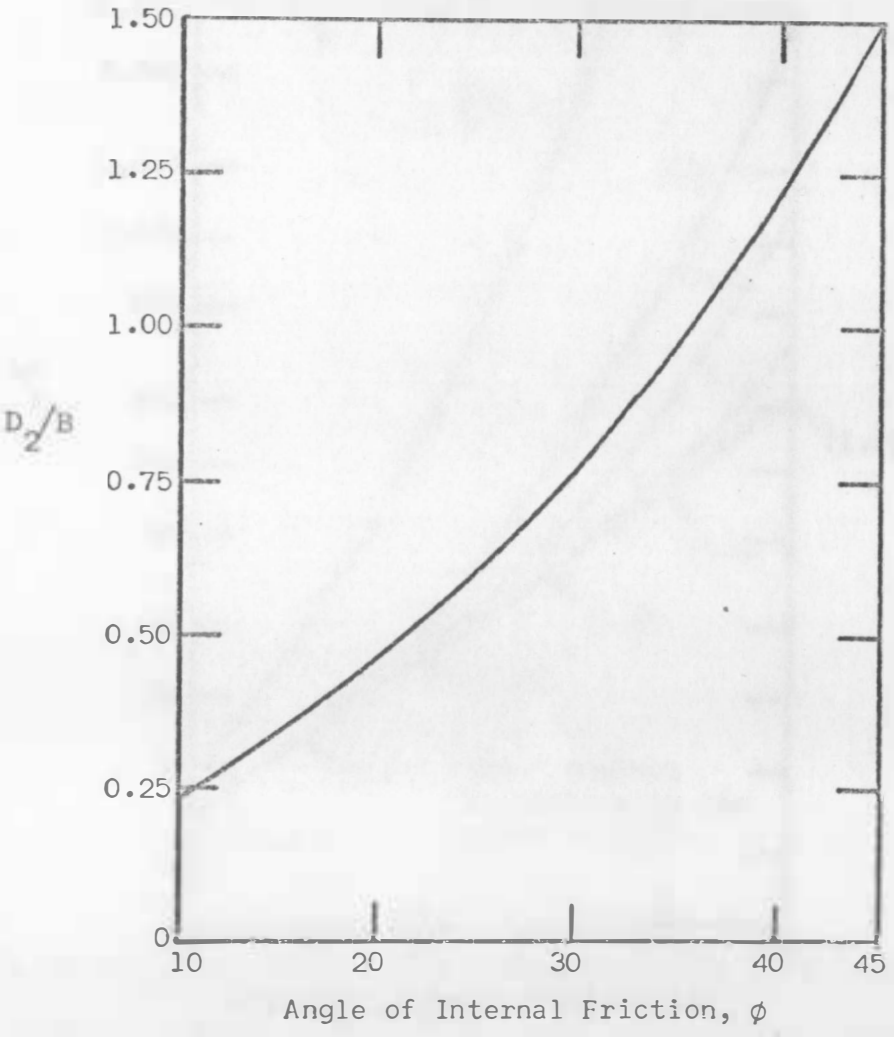

Fig. 2.11. Plot of D_2/B against ϕ.

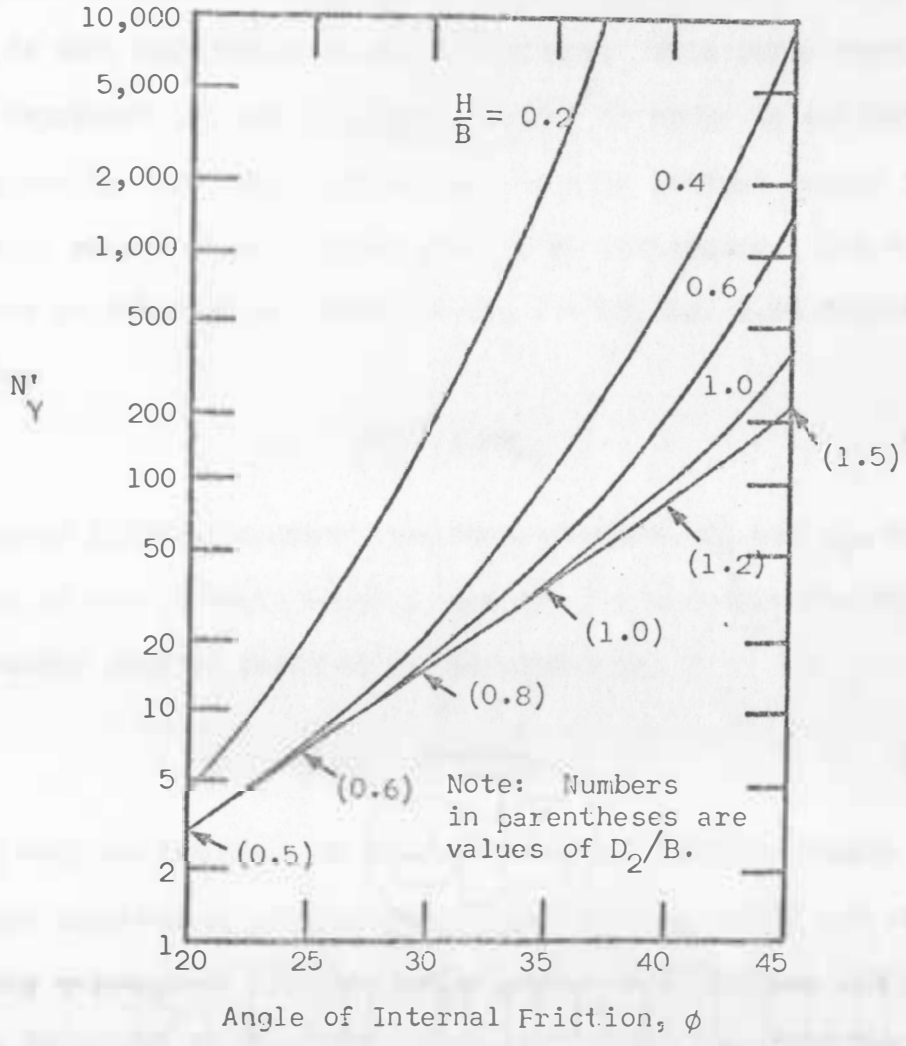

Fig. 2.12. Plot of N'_γ against ϕ (after Meyerhof, 1974, from the numerical values of Mandel and Salencon).

2.4. Ultimate Bearing Capacity for a Rough, Rectangular Foundation Resting on a Granular Soil with a Rough, Rigid Base Located at Shallow Depth

The work of Mandel and Salencon (1972), described in the previous section, is only applicable to strip footings. This strip footing analysis represents a case of plane strain. In order to estimate the bearing capacity for a rectangular footing with limited length to width ratio, proper shape factors need to be introduced. For strip foundations on cohesionless soils (i.e., c = 0), Eq. 2.18 transforms to the form

$$q_u = qN'_q + \tfrac{1}{2}\gamma BN'_\gamma \tag{2.26}$$

Meyerhof (1974) introduced the shape factors, S'_q and S'_γ, for estimation of the ultimate bearing capacity for circular footings. The expression that he obtained can be stated as,

$$q_u = qS'_qN'_q + \tfrac{1}{2}\gamma BS'_\gamma N'_\gamma \tag{2.27}$$

S'_q and S'_γ will be functions of H/B and the soil friction angle. Based on his past theoretical work (Meyerhof and Chaplin, 1953) and with simplifying assumptions that in radial planes the stresses and shear zones are identical to those in transverse planes, Meyerhof has evaluated the approximate values of S'_q and S'_γ.

For rectangular footings, Meyerhof has also proposed the semi-empirical shape factors. These shape factors can be stated as

$$\lambda'_q = [1 - (1 - S'_q)B/L] \tag{2.28}$$

and

$$\lambda'_\gamma = [1 - (1 - S'_\gamma)B/L] \tag{2.29}$$

where B and L are the width and length of the foundation, respectively.

It appears that Eqs. 2.28 and 2.29 can be written in the following simpler form:

$$\lambda'_q = 1 - m_1 B/L \tag{2.30}$$

and

$$\lambda'_\gamma = 1 - m_2 B/L \tag{2.31}$$

where

$$m_1 = 1 - S'_q$$

and

$$m_2 = 1 - S'_\gamma$$

Using the theoretical values of S'_q and S'_γ, the values of m_1 and m_2 have been calculated and are given in Fig. 2.13(a) and (b).

Thus, the general bearing capacity equation for rectangular footings on granular soil may be written as

$$q_u = q\lambda'_q N'_q + \tfrac{1}{2}\gamma B\lambda'_\gamma N'_\gamma \tag{2.32}$$

2.5. Experimental Investigations for Ultimate Capacity for Rough Foundations on Granular Soil with a Rough, Rigid Base Located at Shallow Depth

A limited number of experimental investigations have been conducted in the past to determine the value of N'_γ and N'_q and shape factors in order to compare them with the theory presented in the

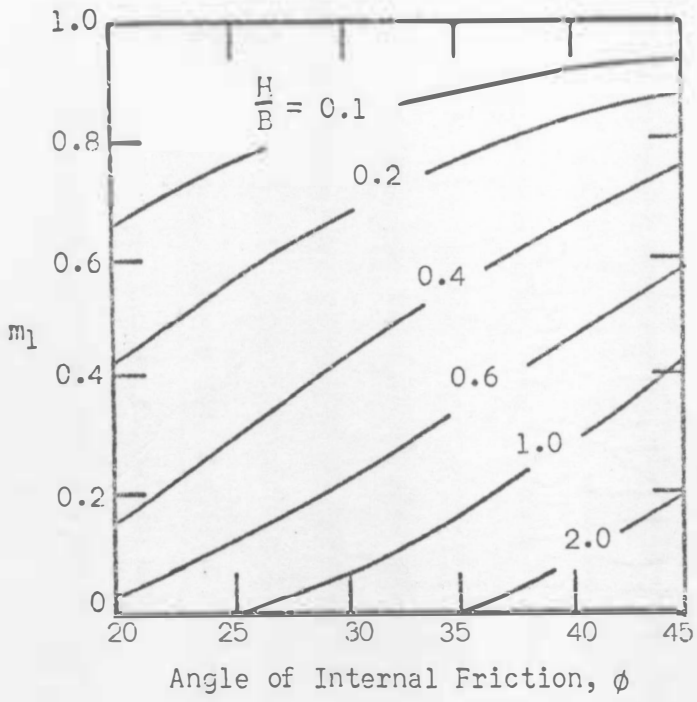

(a)

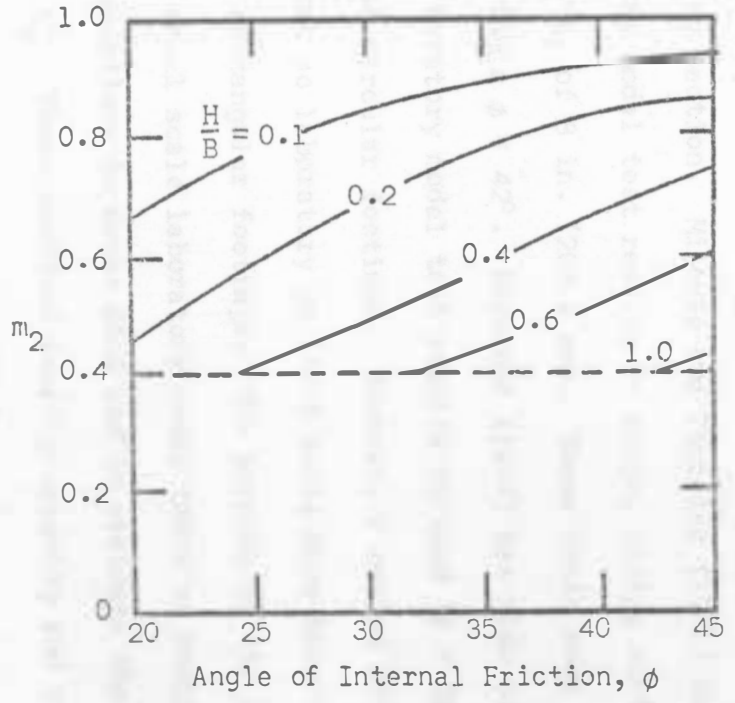

(b)

Fig. 2.13. Plot of m_1 and m_2 for various values of H_1/B and ϕ.

preceeding section. Milovic and Tournier (1971) have reported limited laboratory model test results on rough, strip, surface footings having a width, B, of 8 in. (203.2 mm). These tests were conducted in dense sand having a $\phi = 42^{o}$. Meyerhof (1974) has also presented some small scale laboratory model test results in sand ($\phi = 38^{o}$ and 45^{o}) for rough strip and circular footings. However, a review of existing literature shows that no laboratory or field tests have been conducted in the past on rectangular footings. The purpose of the present study is to conduct small scale laboratory model tests on rough, rectangular, surface foundations in dense sand and to evaluate the modified shape factor, λ'_{γ}. These modified bearing capacity and shape factors will be compared with the existing theories.

CHAPTER III

LABORATORY MODEL TESTS

3.1. General

Small scale model tests were conducted in the laboratory in order to study the effects on the soil bearing capacity for rough, rectangular, shallow foundations due to the existance of a rough, rigid base at shallow depths from the base of the footings. The effects observed also included the settlement of footings at ultimate load. The length-to-width ratio of the footings were varied from one to six. All the model tests conducted in this study were limited to the case of surface footings on cohesionless soils.

3.2. Physical Properties of the Sand Used in the Study

As was mentioned previously, sand was used in all the tests conducted for this investigation. The sand was obtained from the Missouri River near Pollock, South Dakota. Upon arrival to the laboratory, it was sifted through a No. 10 U. S. Standard sieve (opening = 2 mm). The material was then oven dried prior to testing.

Standard tests were conducted to determine the significant properties of the sand. These properties are shown in Table 3.1. The grain-size distribution curve for the sand is given in Fig. 3.1. Examination of the grain-size distribution curve indicated the sand to be fairly uniform with few fine grains present.

TABLE 3.1

CHARACTERISTICS OF THE SAND USED FOR MODEL TEST

% Passing U. S. Sieve No. 10	100
% Passing U. S. Sieve No. 40	27
% Passing U. S. Sieve No. 200	5
Coefficient of Uniformity , C_u	4
Specific Gravity, G_s	2.67
Maximum Dry Density, $\gamma_{d(max)}$	110.75 pcf[a]
Void Ratio at Maximum Density	0.50
Minimum Dry Density, $\gamma_{d(min)}$	93.50 pcf
Void Ratio at Minimum Density	0.78

[a] 1 pcf = 15.95 Kg/m^3

3.3. Description of Model Test Equipment

The model tests were performed in a box measuring 3 ft x 3 ft x 1.5 ft (0.91 m x 0.91 m x 0.46 m). The walls of the box were reinforced using small steel channels. To insure rigidity of the base, 2-inch wood planking was fastened directly to the bottom of the box. This assembly was then placed over a framework of medium-sized channels. In order to obtain a rough base, the inside bottom of the box was covered with a sand-glue mixture. In this case, the sand-glue mixture was spread over a 3 ft x 3 ft masonite panel. After allowing

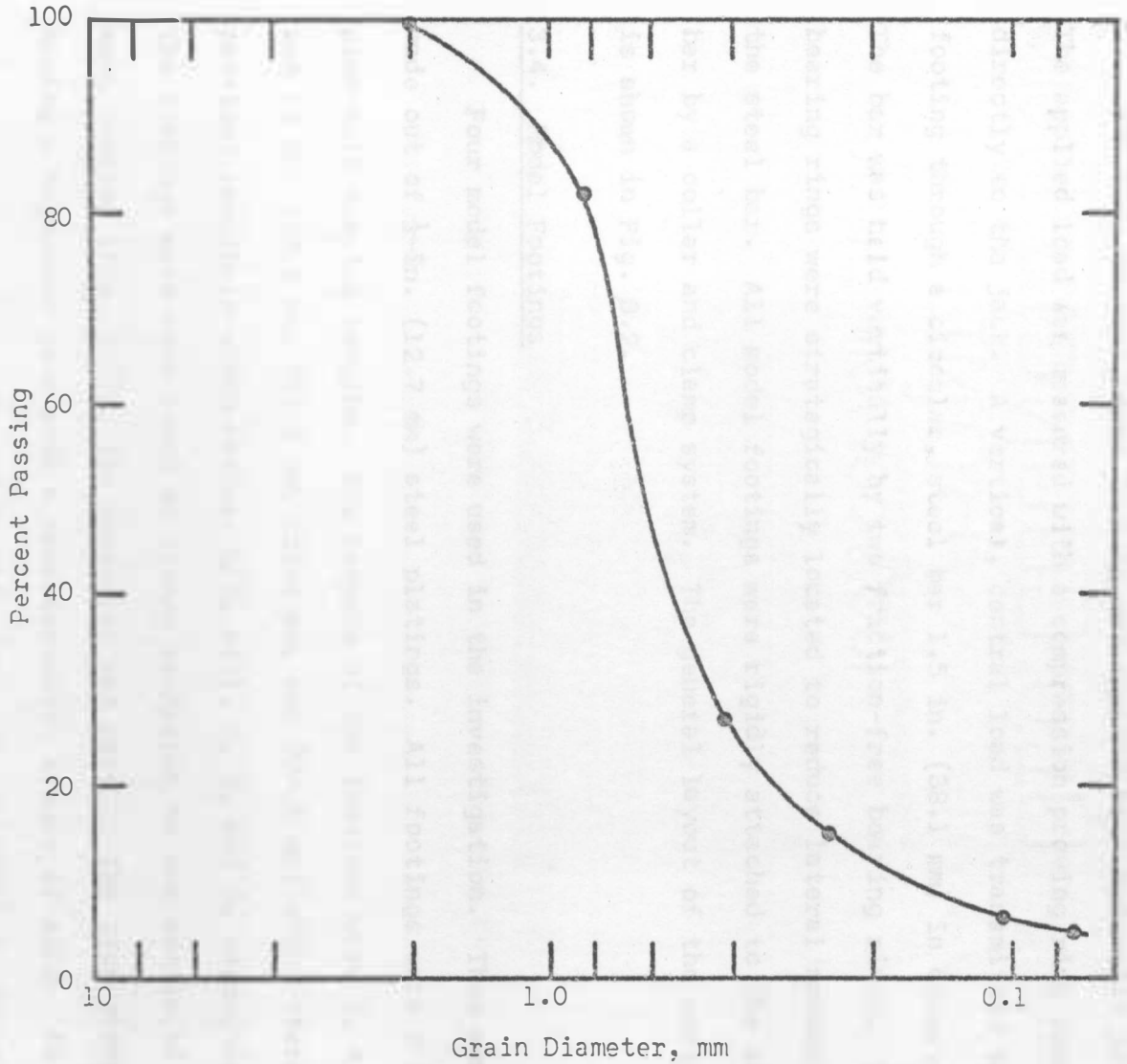

Fig. 3.1. Grain size distribution curve for model study sand.

the mixture to dry, the masonite panel was attached to the bottom of the box with wood screws. The sand used for the sand-glue mixture was identical to the sand used for the model tests.

The load on each model footing was applied by a hydraulic jack. The applied load was measured with a compression proving ring connected directly to the jack. A vertical, central load was transmitted to the footing through a circular, steel bar 1.5 in. (38.1 mm) in diameter. The bar was held vertically by two friction-free bearing rings. These bearing rings were strategically located to reduce lateral movement of the steel bar. All model footings were rigidly attached to the steel bar by a collar and clamp system. The general layout of the equipment is shown in Fig. 3.2.

3.4. Model Footings

Four model footings were used in the investigation. They were made out of $\frac{1}{2}$-in. (12.7 mm) steel platings. All footings were 2 in. wide with varying lengths. The lengths of the footings were 2, 4, 6, and 12 in. (50.8 mm, 101.6 mm, 152.4 mm, and 304.8 mm) which thereby provided length-to-width ratios, L/B, of 1, 2, 3, and 6, respectively. The footings were made rough by gluing sandpaper to the bottom of each footing (Fig. 3.3). The sandpaper was made in the laboratory by mixing a high-bond glue with a representative sample of sand. As with the rough base, the sand used in this case was identical to the sand used to conduct the model tests. This procedure was used to insure that the frictional characteristics of the footing surface and the

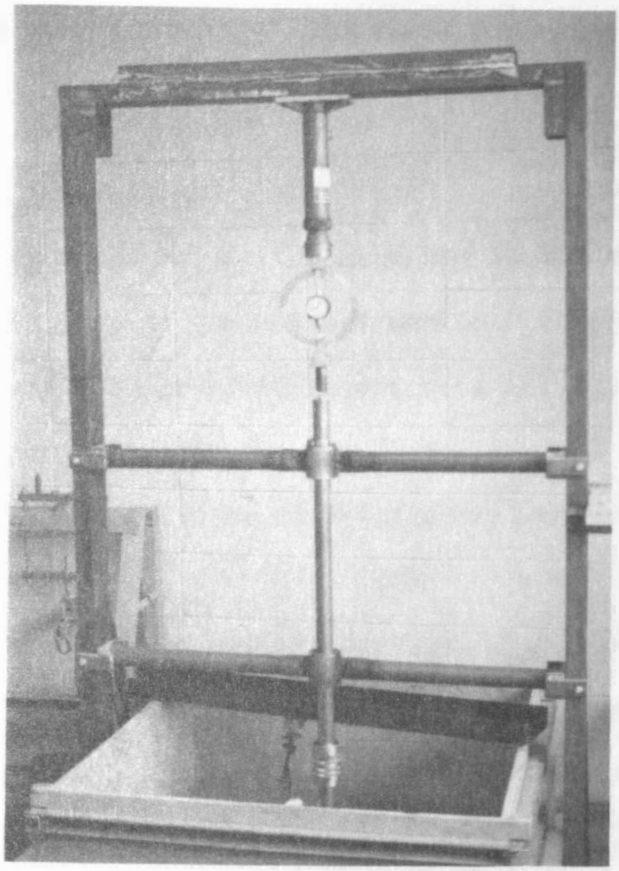

Fig. 3.2. General layout of model test equipment.

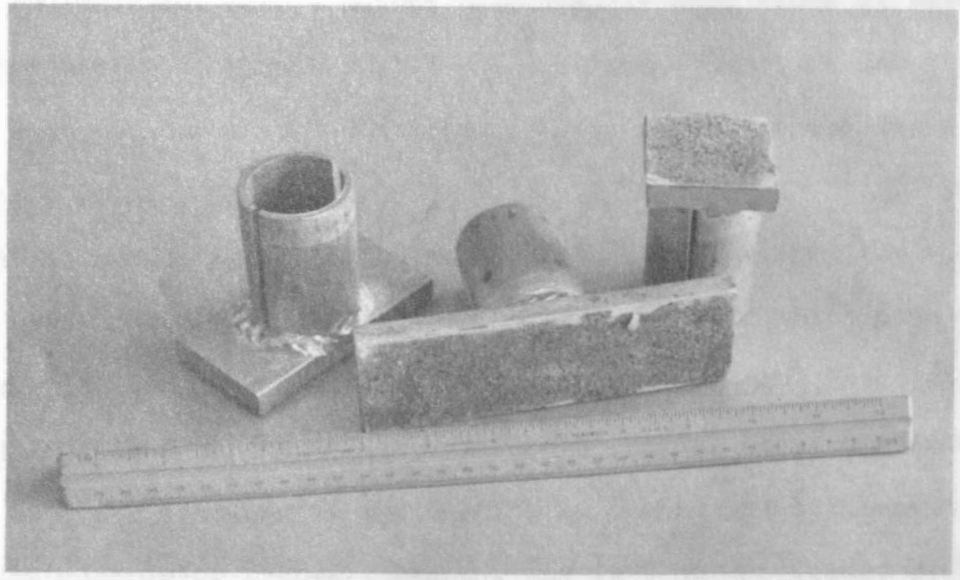

Fig. 3.3. Test footings used in model study.

experimental sand were identical. The sandpaper was dried for several days before experimental use.

3.5. Preparation and Testing

Before testing could begin, the sand had to be compacted to a predetermined density up to the desired depths. To insure uniform compaction, the sand was placed in layers of 1 in. (25.4 mm) or less and uniformly tamped. The density, γ, chosen for all tests was 103.33 pcf. At this density, the angle of friction was determined to be 43 degrees.

In order to achieve the desired density, 77.5 lbs. of sand were placed in the testing box per one inch of height. Compaction was performed by uniformly tamping the sand's surface. Compaction ceased when the height of the sand layer was one inch. This height was determined by placing one-inch scale marks on the inside walls of the box. In addition, sample height measurements were taken at several interior points to insure that a uniform layer thickness was achieved. These measurements were taken from a static plane located above the testing box.

After compaction of the sand had been accomplished, the model tests were conducted. Initially, the footing was permitted to come in contact with the soil in such a manner as to avoid any load transfer from the footing to the soil. After this initial step, a micrometer (Fig. 3.4) was attached to the footing to record the settlement data. With the micrometer properly placed, the footing was loaded by the

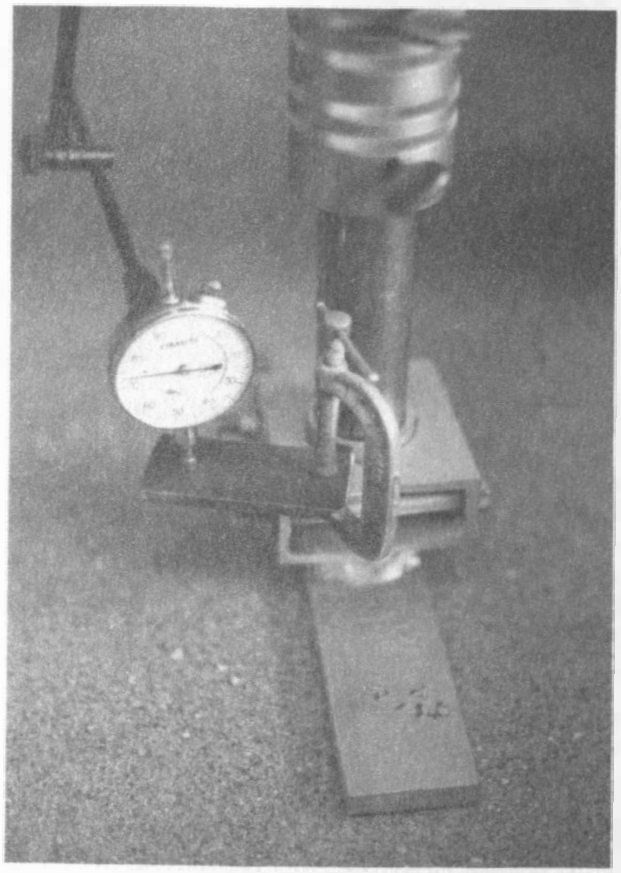

Fig. 3.4. Measurement of footing settlement with micrometer.

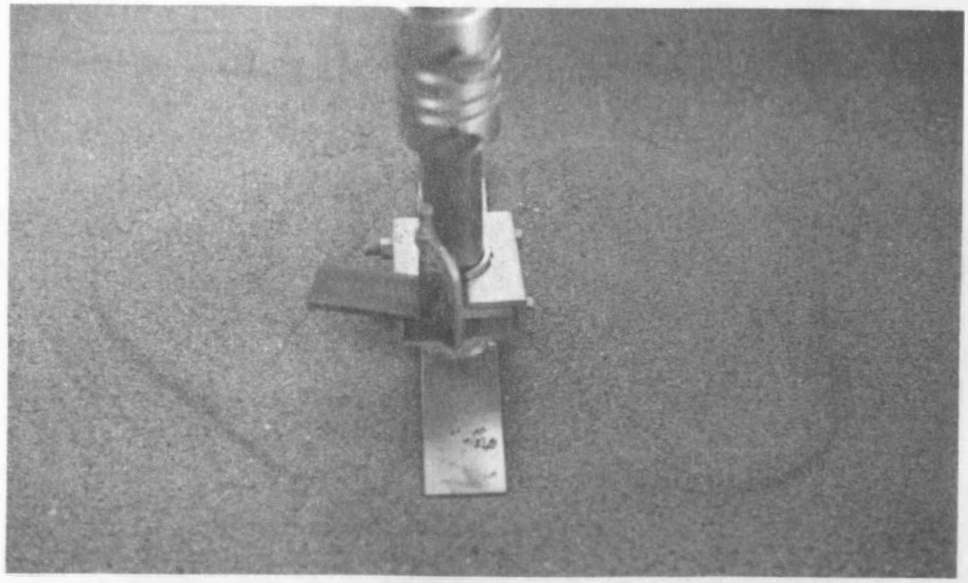

Fig. 3.5. Typical failure pattern for model test.

hydraulic jack. The proving ring dial gauge was read for every 0.01 in. (0.254 mm) of footing settlement. Load application was halted only after the maximum bearing load or an excessive settlement was observed. From this data, load-settlement curves were plotted.

After each test, surface failure patterns were observed. In certain cases, photographs of these failure patterns were taken. An example of a failure pattern is shown in Fig. 3.5. Upon completion of each test, the sand was removed from the box and then recompacted.

CHAPTER IV

MODEL TEST RESULTS AND ANALYSIS

4.1. Evaluation of the Experimental Ultimate Bearing Capacity

As stated in the preceeding chapter, load application to the footings was continued until sudden failure occurred or excessive settlement with small load increments was observed. During load application, the vertical load (in pounds), Q, was recorded for every 0.01 in. (0.0254 mm) of footing settlement. The unit load on each footing at a given settlement can be calculated as

$$q = \frac{Q}{BL} \tag{4.1}$$

where

q = load per unit area of the footing

B = width of the footing,

and

L = length of the footing.

By using the experimental, observed loads, Q, the unit loads, q, for various footing settlements were calculated using Eq. 4.1. Typical q vs. S plots for conditions when the rigid base are located at a limited depth ($\frac{H}{B} \approx 0.4 - 0.50$) is shown in Fig. 4.1. Fig. 4.2 shows the plots of q vs. S for the model plates at $\frac{H}{B} = 3$. This condition represents the rigid base located at great depth.

The ultimate bearing capacity, q_u, was found from an examination of the pressure-settlement diagrams. The ultimate unit load is

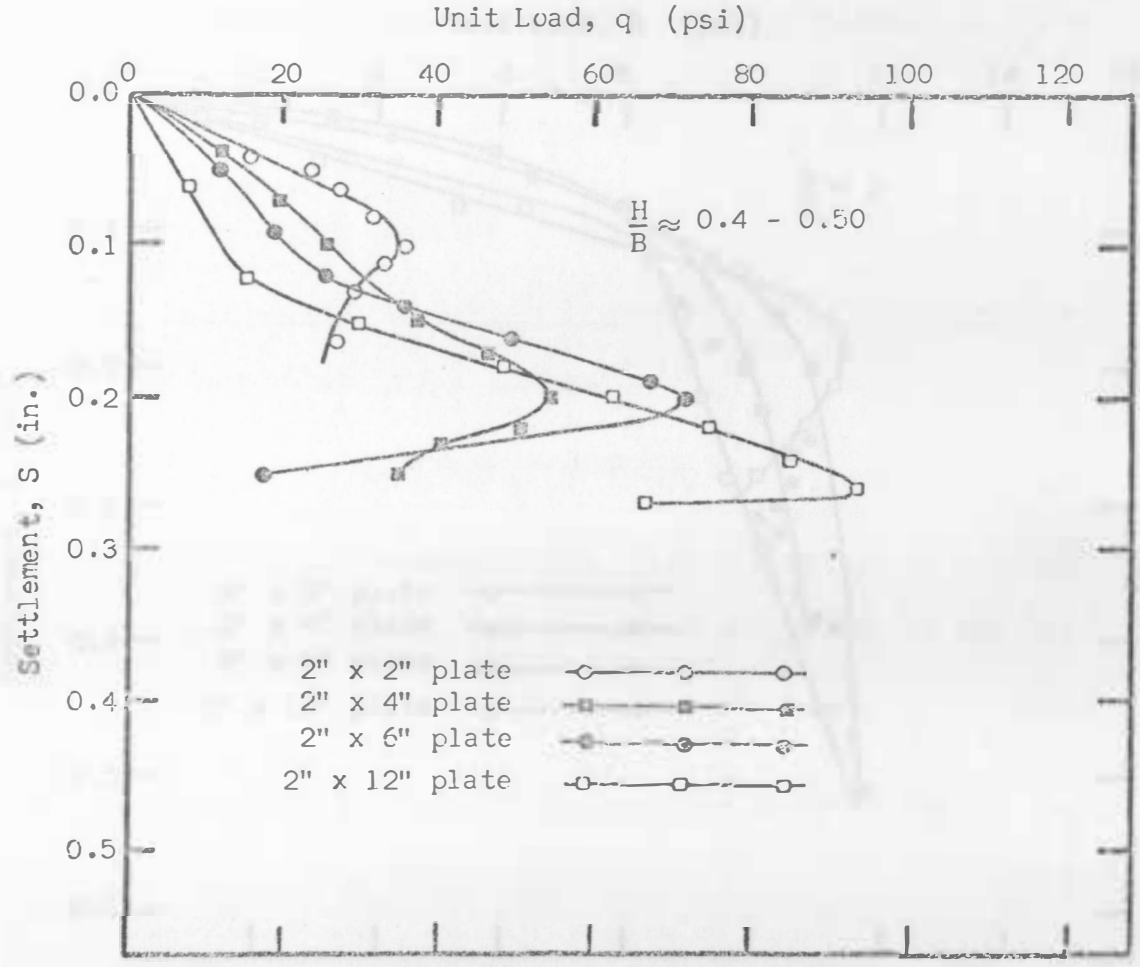

Fig. 4.1. Typical q vs. S plots for conditions when the rigid base is located at a limited depth.

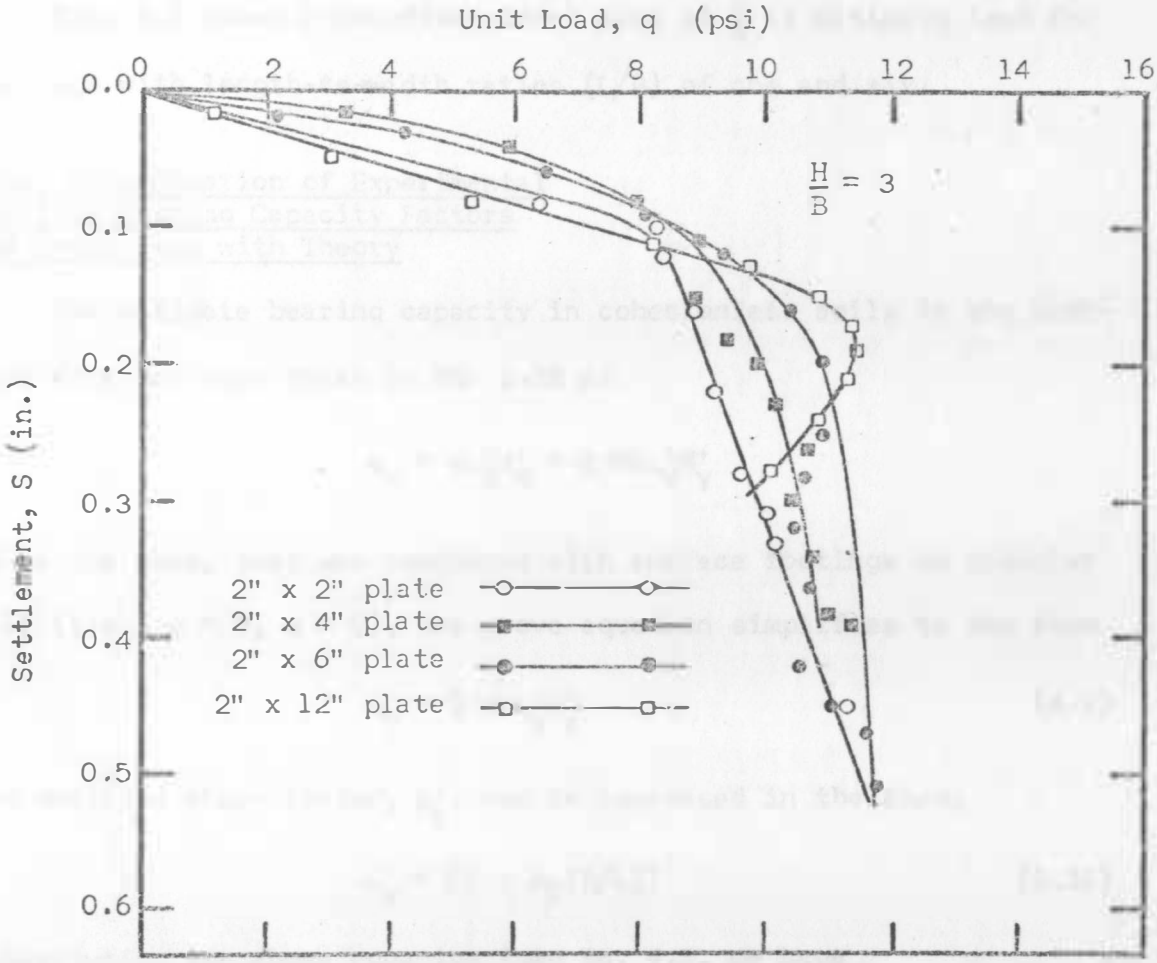

Fig. 4.2. Typical q vs. S plots for conditions when the rigid base is located at great depths.

defined as the point at which the slope of the pressure-settlement curve first reaches zero or a steady, minimum value. The ultimate bearing capacity for the footings under study at various $\frac{H}{B}$ ratios determined by the above procedure is given in Table 4.1.

Fig. 4.3 shows a non-dimensional plot of $\frac{S}{B}$ at ultimate load for footings with length-to-width ratios (L/B) of one and six.

4.2. Determination of Experimental Modified Bearing Capacity Factors and Comparison with Theory

The ultimate bearing capacity in cohesionless soils in the modified form has been given in Eq. 2.32 as

$$q_u = q\lambda'_q N'_q + \tfrac{1}{2}\gamma B \lambda'_\gamma N'_\gamma$$

Since the model test was conducted with surface footings on granular soil (i.e., c = 0, q = 0), the above equation simplifies to the form

$$q_u = \tfrac{1}{2}\gamma B \lambda'_\gamma N'_\gamma \qquad (4.2)$$

The modified shape factor, λ'_γ, can be expressed in the form,

$$\lambda'_\gamma = [1 - m_2(B/L)] \qquad (2.31)$$

Substituting the above equation into Eq. 4.2, we have

$$q_u = \tfrac{1}{2}\gamma B[1 - m_2(B/L)]N'_\gamma$$

or

$$\frac{q_u}{0.5\gamma B} = [1 - m_2(B/L)]N'_\gamma \qquad (4.3)$$

TABLE 4.1

$q_u/0.5\gamma B$ VALUES FOR VARIOUS FOOTING DIMENSIONS WITH CHANGING SOIL DEPTHS*

Footing Size						
Width, B in inches	Length, L in inches	$\frac{B}{L}$	Soil Depth, D in inches	$\frac{D}{B}$	q_u in psi	$\frac{q_u}{0.5\gamma B} = \lambda_\gamma' N_\gamma'$
(1)	(2)	(3)	(4)	(5)	(6)	(7)
2	12	.167	10.0	5.0	11.5	192.3
2	12	.167	6.0	3.0	11.4	191.7
2	12	.167	3.0	1.5	17.9	298.8
2	12	.167	2.37	1.19	22.9	380.9
2	12	.167	1.89	0.95	30.8	514.7
2	12	.167	1.45	0.73	40.1	671.1
2	12	.167	0.85	0.43	93.8	1,569.2
2	6	.333	10.0	5.0	10.7	178.9
2	6	.333	6.0	3.0	11.0	183.9
2	6	.333	3.0	1.5	16.0	267.6
2	6	.333	2.42	1.21	22.7	379.6
2	6	.333	1.92	0.96	31.5	526.8
2	6	.333	1.46	0.73	38.0	634.8
2	6	.333	0.95	0.48	70.8	1,201.3
2	4	.50	10.0	5.0	8.5	141.3
2	4	.50	6.0	3.0	9.5	158.9
2	4	.50	3.0	1.5	15.0	251.3
2	4	.50	2.41	1.21	22.6	377.9
2	4	.50	1.89	0.95	27.8	464.9
2	4	.50	1.42	0.71	33.1	552.7
2	4	.50	0.89	0.54	54.4	909.5

Table 4.1. Continued.

(1)	(2)	(3)	(4)	(5)	(6)	(7)
2	2	1.0	10.0	5.0	7.9	131.2
2	2	1.0	6.0	3.0	8.0	133.4
2	2	1.0	3.0	1.5	10.7	178.3
2	2	1.0	2.46	1.23	15.1	251.8
2	2	1.0	1.89	0.95	20.8	347.0
2	2	1.0	1.44	0.72	19.4	324.3
2	2	1.0	0.89	0.45	35.5	593.7

*1" = 25.4 mm 1 psi = 6.9 KN/m^2

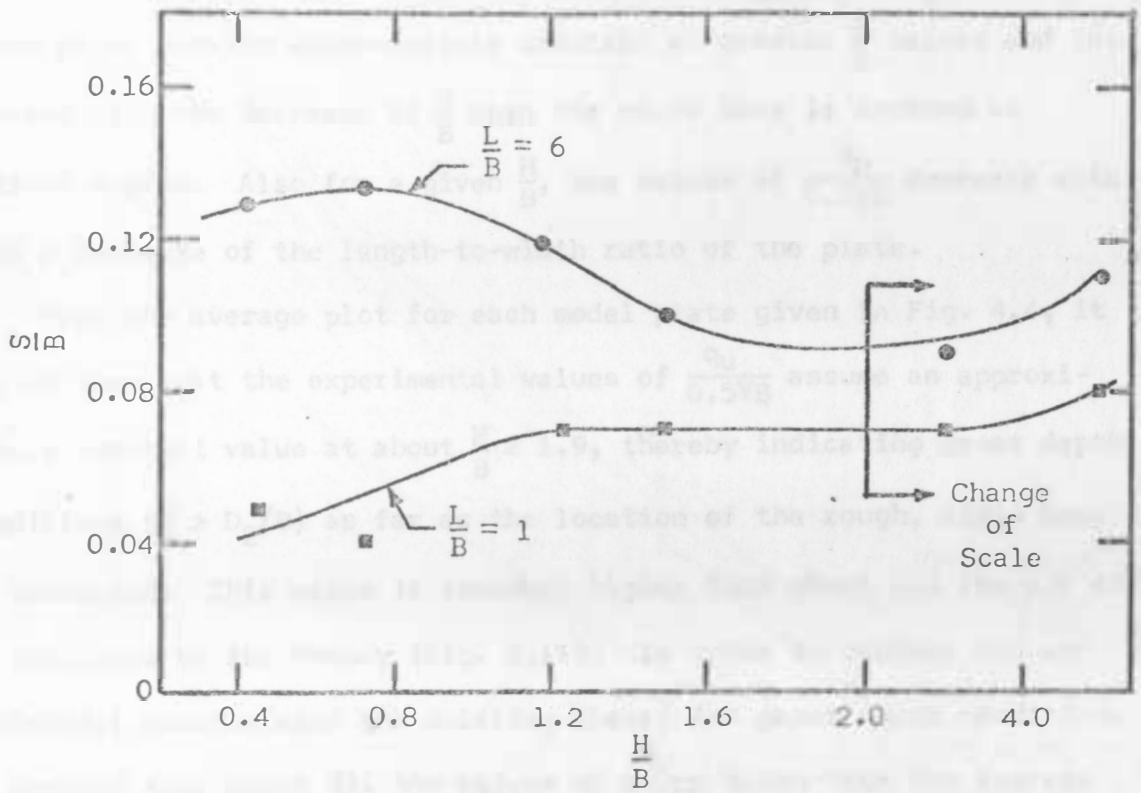

Fig. 4.3. Non-dimensional plot of $\frac{S}{B}$ at ultimate load for footings with length-to-width ratios of one and six.

Using the experimental ultimate bearing capacity, q_u, the values of $\frac{q_u}{0.5\gamma B}$ have been determined and are given in Table 4.1.

The values of $\frac{q_u}{0.5\gamma B}$ given in Column 7 of Table 4.1 for the four plates are plotted against their corresponding $\frac{H}{B}$ ratios in Fig. 4.4. As expected, the general nature of the graph of $\frac{q_u}{0.5\gamma B}$ vs. $\frac{H}{B}$ for any given plate remains approximately constant at greater $\frac{H}{B}$ values and increases with the decrease of $\frac{H}{B}$ when the rigid base is located at limited depths. Also for a given $\frac{H}{B}$, the values of $\frac{q_u}{0.5\gamma B}$ decrease with with a decrease of the length-to-width ratio of the plate.

From the average plot for each model plate given in Fig. 4.4, it may be seen that the experimental values of $\frac{q_u}{0.5\gamma B}$ assume an approximately constant value at about $\frac{H}{B} \geq 1.9$, thereby indicating great depth conditions ($\frac{H}{B} \geq D_2/B$) as far as the location of the rough, rigid base is concerned. This value is somewhat higher than about 1.4 for $\phi = 43^\circ$ as predicted by the theory (Fig. 2.11). In order to compare the experimental results with the existing theory for great depth conditions ($\frac{H}{B}$ greater than about 2), the values of $\frac{q_u}{0.5\gamma B}$ taken from the average plots in Fig. 4.4 are plotted against B/L of the plates along with the theoretical values predicted by Eq. 4.3 (for $\phi = 43^\circ$ and 45°) in Fig. 4.5. It may be noted that for great depths, the theoretical value of m_2 in Eq. 4.3 is equal to 0.4 and N'_γ is equal to N_γ as obtained by the Lundgren and Mortensen procedure. The comparison shows that the experimental values are actually in closer agreement with $\phi = 45^\circ$. This

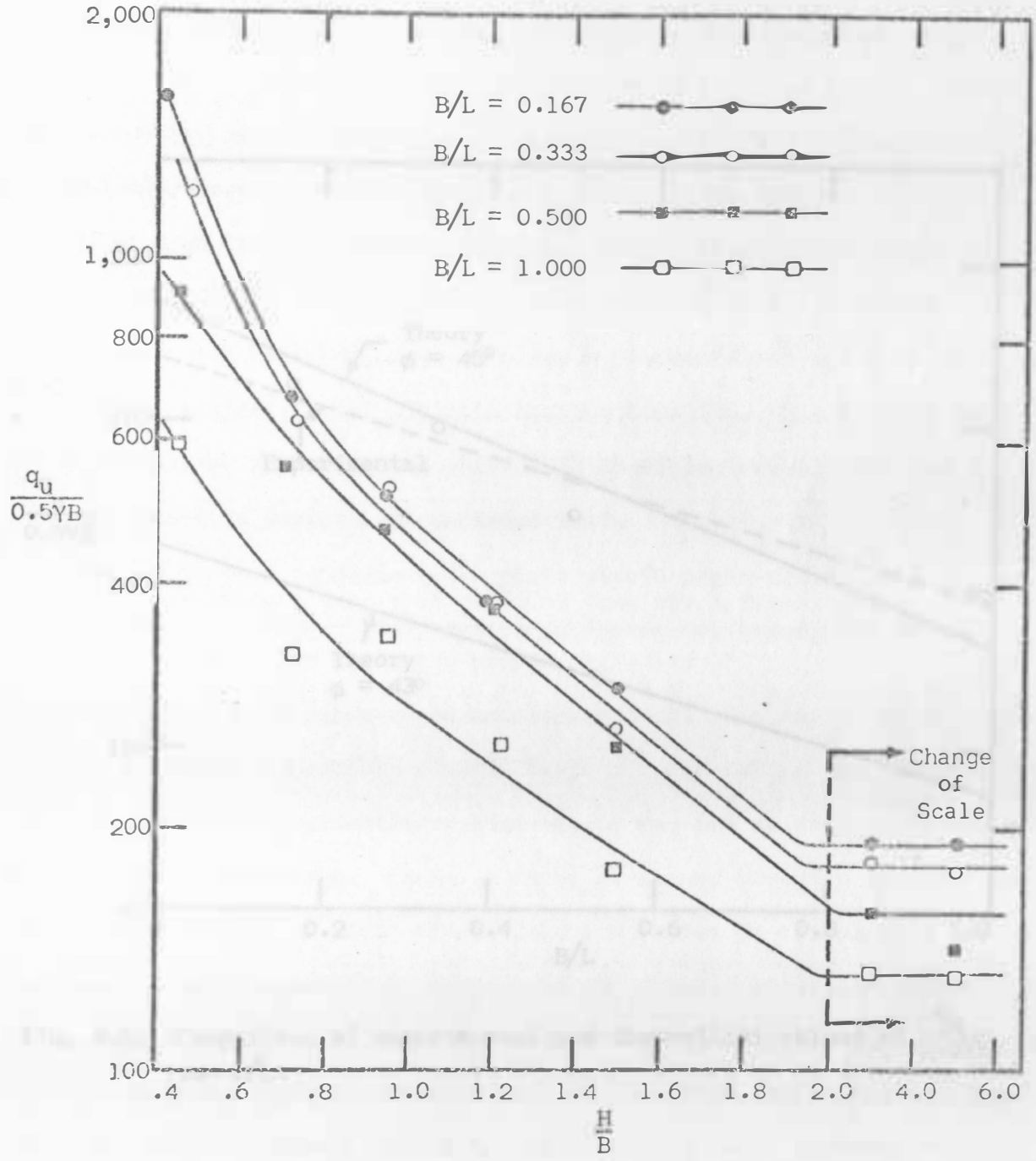

Fig. 4.4. Experimental values of $\frac{q_u}{0.5\gamma B}$ vs. $\frac{H}{B}$ for various length-to-width ratios.

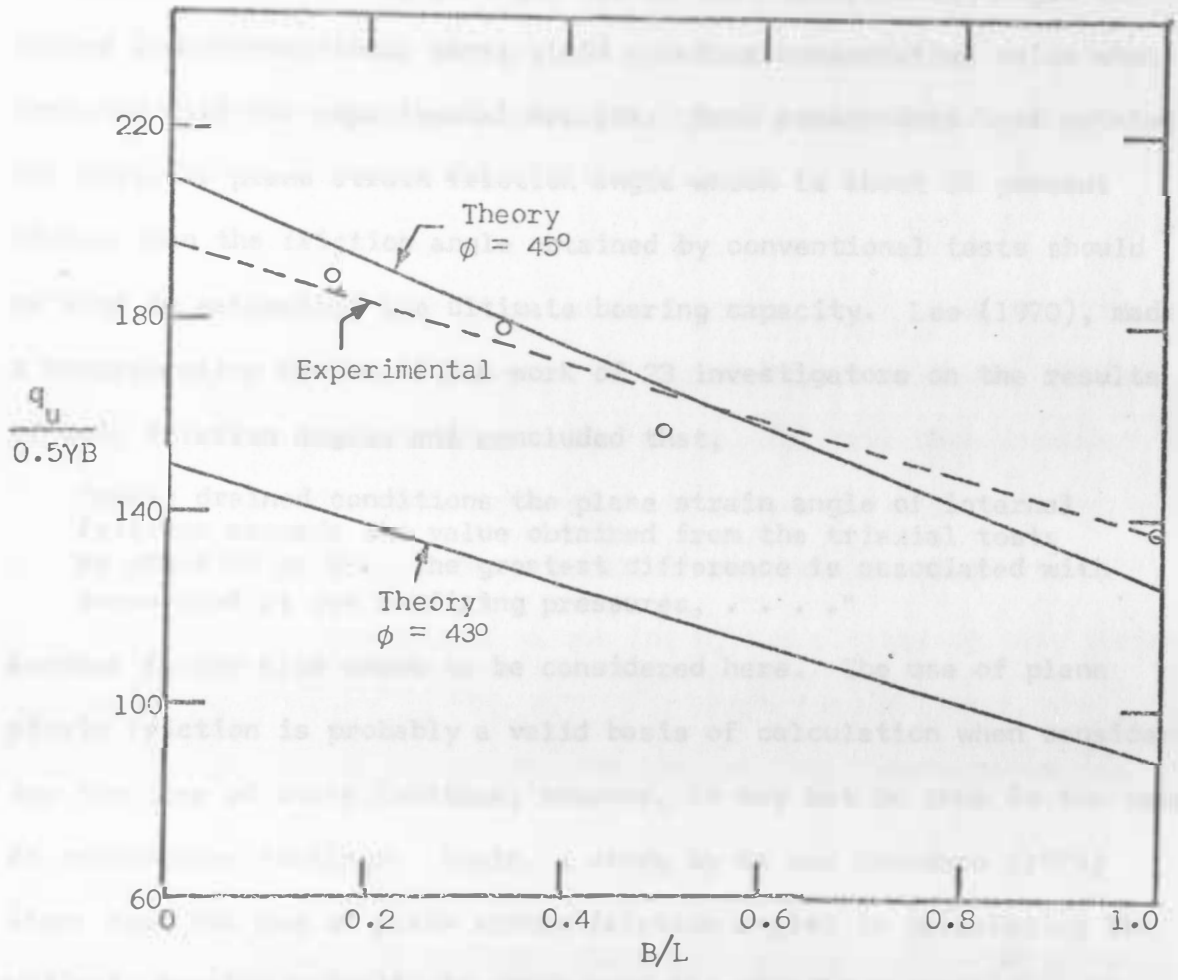

Fig. 4.5. Comparison of experimental and theoretical values of $\frac{q_u}{0.5\gamma B}$ vs. B/L.

result was rather expected and has been a point of discussion among the researchers in the area of bearing capacity for some time. Several investigators have shown that the use of the soil friction angle obtained from conventional tests yield a rather conservative value when compared with the experimental results. Some researchers have pointed out that the plane strain friction angle which is about 10 percent higher than the friction angle obtained by conventional tests should be used in estimating the ultimate bearing capacity. Lee (1970), made a comprehensive review of the work of 23 investigators on the results of soil friction angles and concluded that,

> "under drained conditions the plane strain angle of internal friction exceeds the value obtained from the triaxial tests by about 6° or 8°. The greatest difference is associated with dense sand at low confining pressures, ..."

Another factor also needs to be considered here. The use of plane strain friction is probably a valid basis of calculation when considering the case of strip footings; however, it may not be true in the case of rectangular footings. Again, a study by Ko and Davidson (1973) shows that the use of plane strain friction angles in calculating the ultimate bearing capacity in dense sand may grossly overestimate the actual results. This is probably the case here. Although the plane strain friction angle of the sand used for the model tests has not been determined, if we assume that ϕ (plane strain) = 1.1 ϕ (conventional), then our friction angle will be in the range of about 48°. Use of this friction angle in Eq. 4.3 will give a much higher value than that observed in the model tests.

The values of $\frac{q_u}{0.5\gamma B}$ taken from the average experimental plots given in Fig. 4.4 at $\frac{H}{B}$ = 0.4, 0.6, 0.8, 1.0, 1.2, 1.5, 1.8, and 2 to 5 are plotted against the width-to-length ratios of the plate in Fig. 4.6(a) and 4.6(b). From the plot it can be seen that for a given $\frac{H}{B}$, the variation of $\frac{q_u}{0.5\gamma B}$ against B/L is approximately linear. This result is in general agreement with the nature of the plot as predicted by the theory (i.e., Eq. 4.3). It may also be noticed from Eq. 4.3 that when $B/L \rightarrow 0$ (i.e., strip footings), $\frac{q_u}{0.5\gamma B} \rightarrow N'_\gamma$. Thus, to extrapolate the bearing capacity factors, N'_γ, at various $\frac{H}{B}$ ratios, the linear plots given in Fig. 4.6(a) and 4.6(b) have been produced back to B/L = 0. The intercepts of these linear plots are the deduced modified bearing capacity factors, N'_γ, at various $\frac{H}{B}$ ratios.

The deduced experimental values for N'_γ are plotted against their corresponding $\frac{H}{B}$ values in Fig. 4.7. For comparison purposes, the theoretical values of the modified bearing capacity factors are also plotted in Fig. 4.7 for $\phi = 42^o$, 43^o, and 45^o. These theoretical values of N'_γ are taken from Fig. 2.12. It can be seen that in the region of $0.5 < \frac{H}{B} < 1.9$, the experimentally deduced values of N'_γ are higher than those predicted by the theory for $\phi = 43^o$. Furthermore, they are also higher than the values obtained from the use of the theory of plasticity for $\phi = 45^o$, which is the assumed value for the friction angle that gave a correct estimation of the ultimate bearing capacity for conditions when the rigid base is located at great depths.

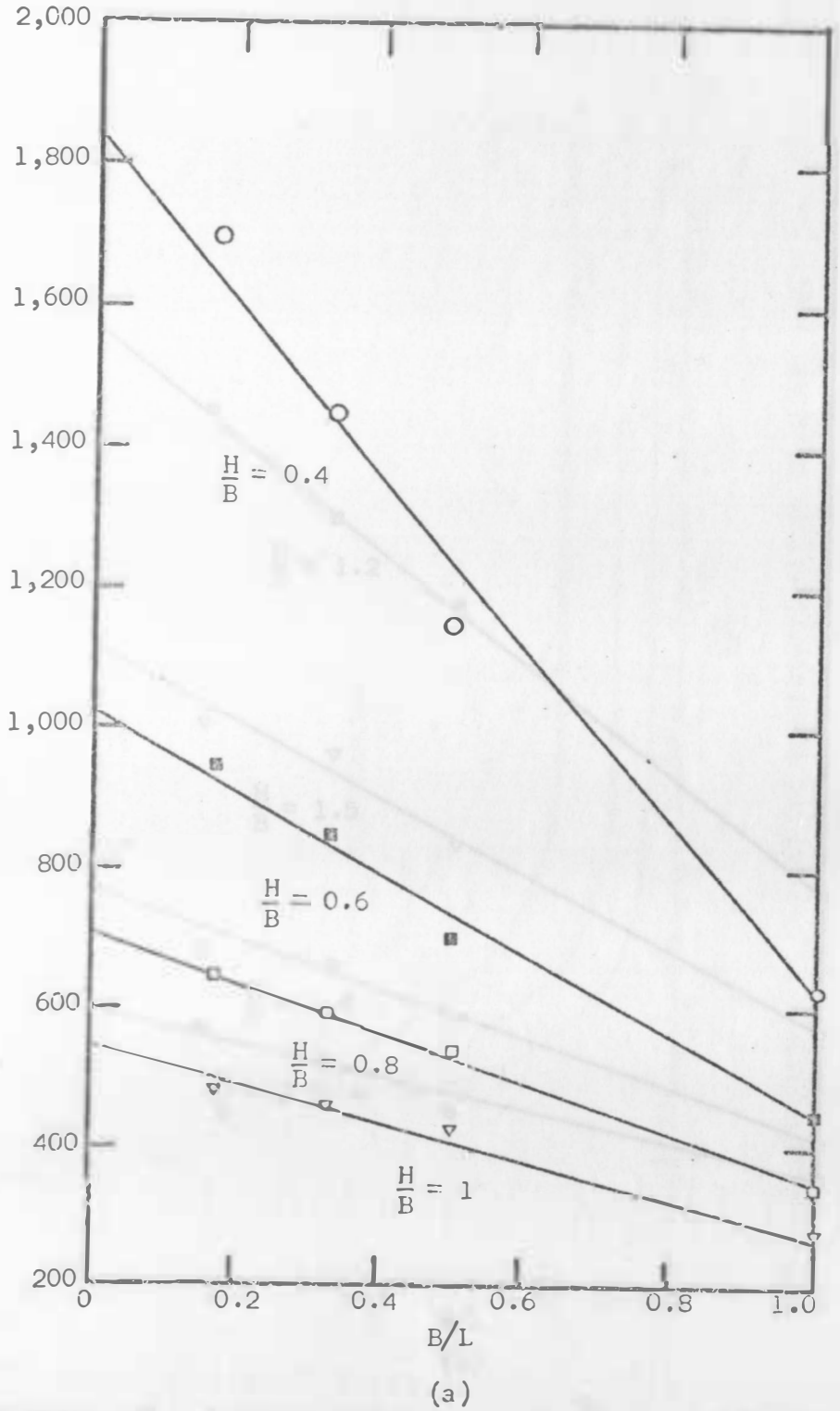

(a)

Fig. 4.6. Experimental values of $\frac{q_u}{0.5\gamma B}$ vs. B/L for various $\frac{H}{B}$ ratios.

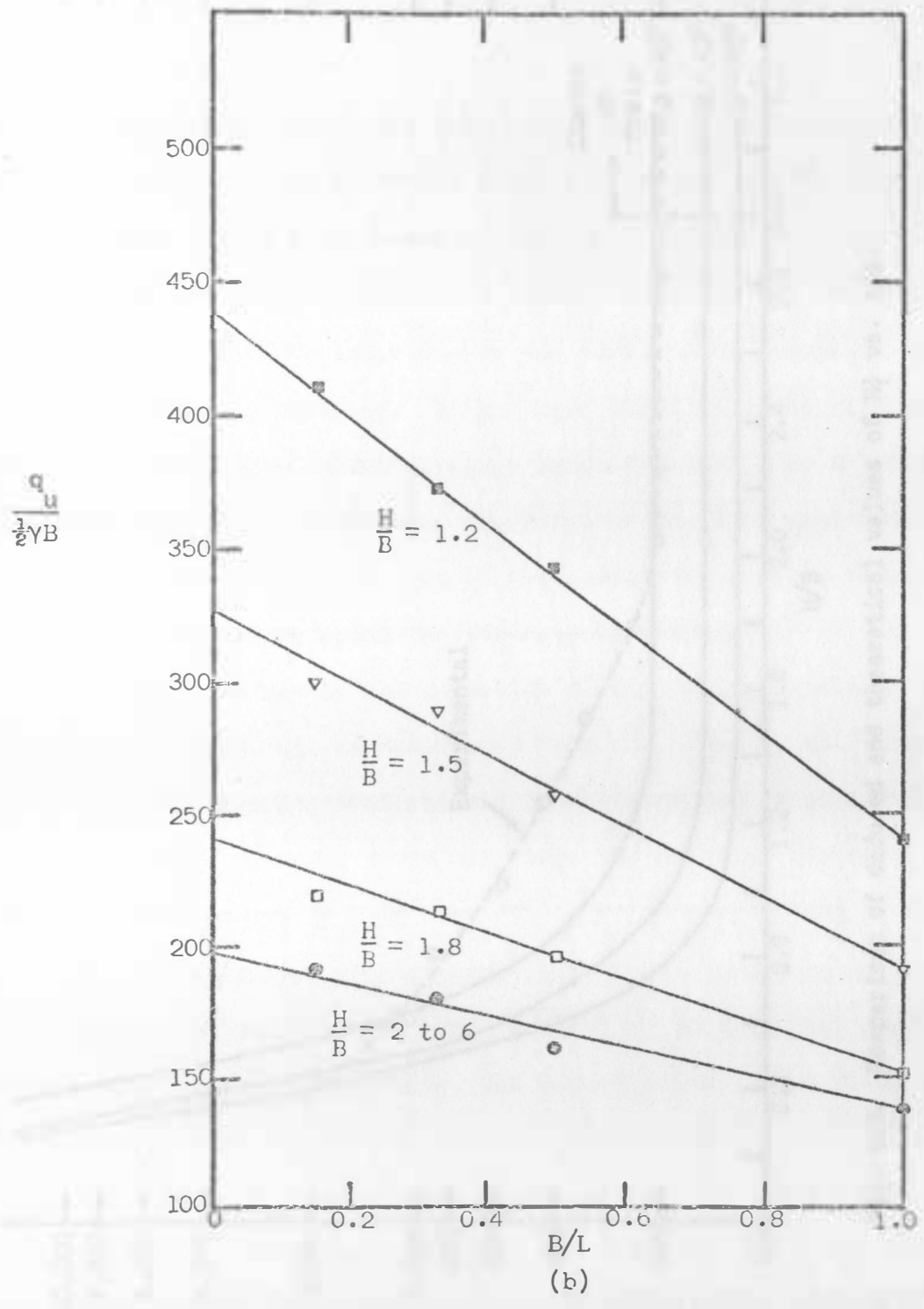

Fig. 4.6. (Continued). Experimental values of $\frac{q_u}{0.5\gamma B}$ vs. B/L for various $\frac{H}{B}$ ratios.

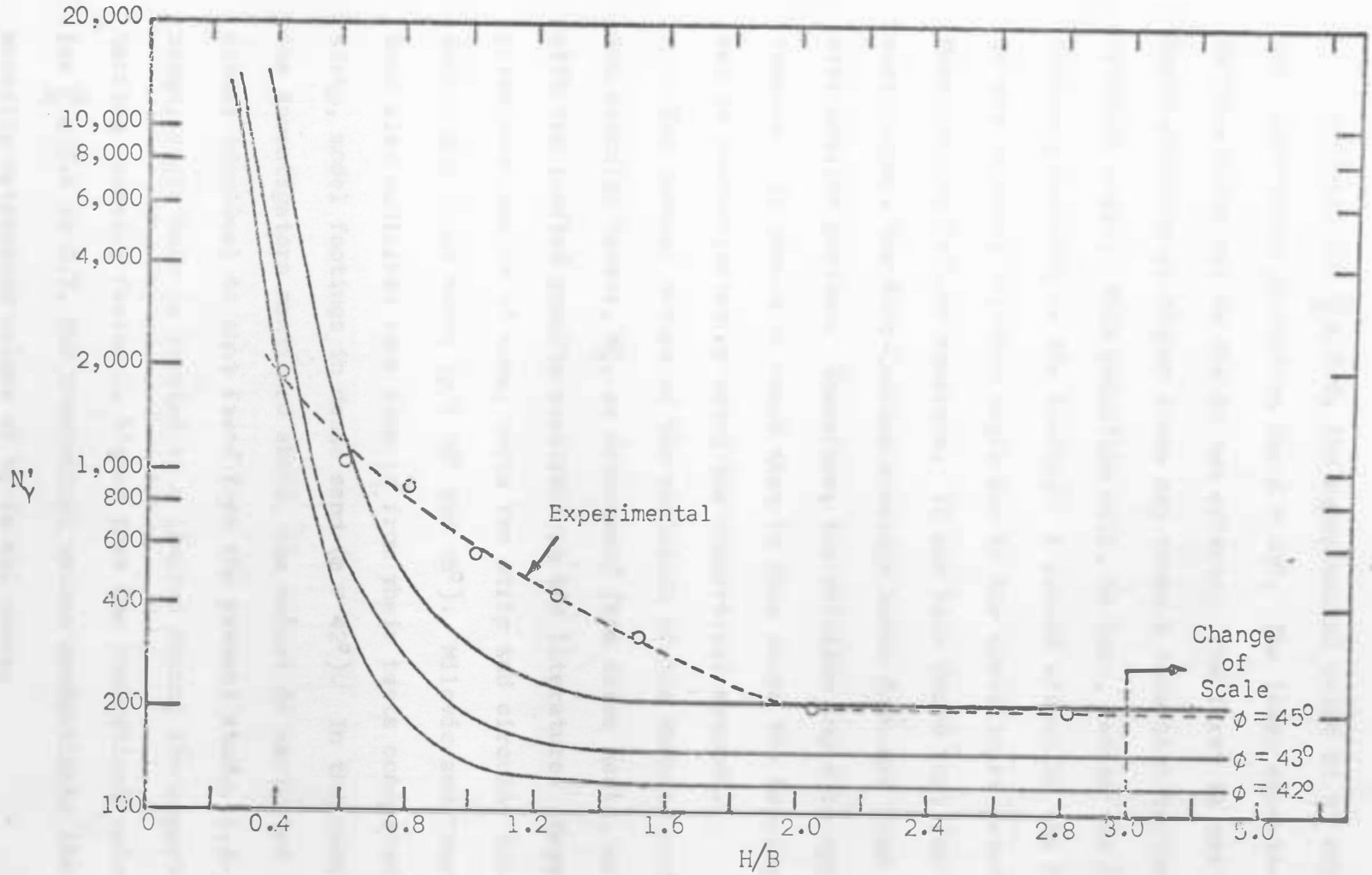

Fig. 4.7. Comparison of deduced and theoretical values of N'_γ vs. H/B.

However, for $\frac{H}{B} < 0.5$, the experimental value of N'_γ drops below the theoretical prediction for $\phi = 43^\circ$. The lower experimental values in this range may be due to two effects. The first is grain crushing. Grain crushing at higher loads may cause a reduction in the internal friction angle. This reduction will, in turn, reduce the load-carrying capacity of the footing. A second effect is the reduction of the internal friction angle due to the curvilinear nature of the Mohr-Coulomb failure envelope. It has been found that for high pressure ranges, the Mohr-Coulomb envelope bends downward from the assumed straightline portion. Therefore, the friction angle is apparently reduced. It should be noted that in this range the bearing capacity may be overestimated by using the theoretical methods.

The general nature of the variation of the deduced modified bearing capacity factor, N'_γ, as determined from these tests, was compared with the limited results available in the literature. Meyerhof (1974) presented results of model tests for strip and circular footings in medium and dense sands ($\phi = 38^\circ$ and 45°). Milovic and Tournier (1971) have also published some results from their tests conducted on rough, strip, model footings in dense sand ($\phi = 42^\circ$). In the model tests by the investigators mentioned above, the nature of variation of N'_γ is almost identical to that found from the present study, i.e., when the rough, rigid base is located at a limited depth, the experimental bearing capacity factor is higher than the theoretical value. However, for $\frac{H}{B} \leq 0.4$ to 0.7, the theoretical values overestimate the experimentally determined values of N'_γ in all cases.

4.3. Modified Bearing Shape Factor

From Eq. 4.3, for rectangular footings,

$$\frac{q_u}{0.5\gamma B} = [1 - m_2(B/L)]N'_\gamma$$

Referring to Fig. 4.6(a) and 4.6(b), it may be seen that the nature of variation of $\frac{q_u}{0.5\gamma B}$ for rectangular footings (for a given $\frac{H}{B}$) is approximately linear as predicted by Eq. 4.3. However, in order to compare the magnitude of the experimental m_2 with those predicted by Meyerhof's approximate theory, the following procedure was adopted. For the strip footing case, B/L = 0. So, from Eq. 4.3

$$\left[\frac{q_u}{0.5\gamma B}\right]_{B/L = 0} = N'_\gamma \tag{4.4}$$

Similarly, for the square footing case, B/L = 1 and Eq. 4.3 for this case yields

$$\left[\frac{q_u}{0.5\gamma B}\right]_{B/L = 1} = N'_\gamma [1 - m_2] \tag{4.5}$$

So, from Eqs. 4.4 and 4.5,

$$\frac{\left[\frac{q_u}{0.5\gamma B}\right]_{B/L = 1}}{\left[\frac{q_u}{0.5\gamma B}\right]_{B/L = 0}} = [1 - m_2]$$

or

$$m_2 = 1 - \frac{\left[\frac{q_u}{0.5\gamma B}\right]_{B/L = 1}}{\left[\frac{q_u}{0.5\gamma B}\right]_{B/L = 0}} \tag{4.6}$$

Using the values of $\left[\frac{q_u}{0.5\gamma B}\right]_{B/L = 0}$ and $\left[\frac{q_u}{0.5\gamma B}\right]_{B/L = 1}$ from the linear plots of Fig. 4.6(a) and 4.6(b), the values of m_2 are shown in Fig. 4.8. The theoretical values of m_2 for $\phi = 43^{\circ}$ are also plotted for comparative purposes. These values are taken from Fig. 2.13(b). When the rigid base is located at great depths (i.e., H greater than about 1.9 times the width of the footing as found from these tests), the experimental value of m_2 is about 0.32 as compared to the theoretical prediction of 0.4. For the case when the rough, rigid base is located at shallow depths, i.e., $\frac{H}{B} < 1.9$, the overall variation of m_2 is from about -0.06 to +0.08. Taking into consideration the real soil behavior and the theoretical assumptions involved in soil mechanics, it can be concluded that the agreement between the experimental and theoretical values is good.

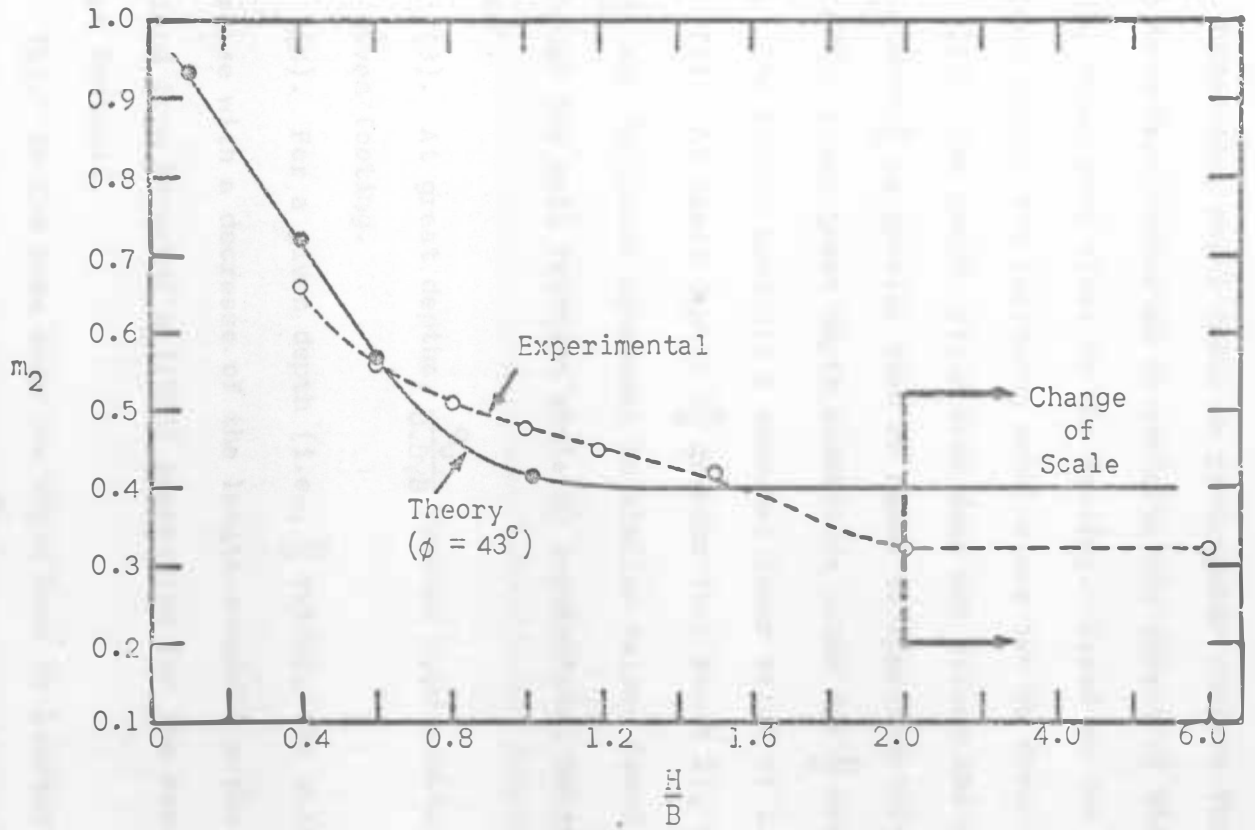

Fig. 4.8. Comparison of experimental and theoretical values of m_2 vs. $\frac{H}{B}$.

CHAPTER V

CONCLUSIONS

Laboratory model tests on rectangular surface footings in dense sand have been conducted to evaluate the effect of the location of a rough, rigid base close to the footing. Based on the findings of the present study, the following conclusions can be drawn:

(1). The rough, rigid base does not affect the values of $\frac{q_u}{0.5\gamma B}$ when $\frac{H}{B}$ is greater than or equal to approximately 1.9 for $\phi = 43^\circ$. Thus, great depth conditions occur for $\frac{H}{B}$ values higher than 1.9. The theory predicts a somewhat lower value of 1.4.

(2). At great depths ($\frac{H}{B}$ greater than about 2), the values of $\frac{q_u}{0.5\gamma B}$ are in closer agreement to similar values found by using $\phi = 45^\circ$, although the soil friction angle by conventional tests was found to be 43°.

(3). At great depths, $\frac{q_u}{0.5\gamma B}$ remains approximately constant for any given footing.

(4). For a given depth (i.e., $\frac{H}{B}$ ratio), the values of $\frac{q_u}{0.5\gamma B}$ decrease with a decrease of the length-to-width ratio. This result is implied from Meyerhof's (1974) expression for the bearing capacity shape factors.

(5). In the case when the rigid base is located at a limited depth ($\frac{H}{B} < 1.9$), the values of $\frac{q_u}{0.5\gamma B}$ increase with the decrease of $\frac{H}{B}$. This result was predicted from the theoretical analysis of Mandel and Salencon (1969).

(6). For a given $\frac{H}{B}$, the variation of $\frac{q_u}{0.5\gamma B}$ with B/L is approximately linear. This result is in general agreement with the theoretical analysis presented by Meyerhof (1974).

(7). In the region of $0.5 < \frac{H}{B} < 1.9$, the values of the modified bearing capacity factor, N'_γ, are higher than those predicted by the theory for $\phi = 43^o$. In addition, they are also higher than the values for $\phi = 45^o$, which is the assumed value for the friction angle that gave a correct estimation of the ultimate bearing capacity for conditions when the rigid base is located at great depths. Thus, the theoretical values of N'_γ appear to be conservative in this region.

(8). For $\frac{H}{B} < 0.5$, the deduced values of N'_γ are less than those predicted by theory for $\phi = 43^o$. Examination of the experimental work of Meyerhof (1974) and Milovic and Tournier (1971), also shows similar trends. Thus, the theoretical values for N'_γ appear to cause an overestimation of the ultimate bearing capacity in this region. This result may be attributed to an actual decrease of the internal friction angle due to the effects of grain crushing.

(9). The experimental value of m_2 is found to be equal to 0.32 when the rigid base is at great depths. The theory predicts a value of 0.4 for m_2.

(10). For $\frac{H}{B}$ values less than 1.9 (i.e., rigid base at a limited depth), the variation of m_2 is about -0.06 to +0.08. This variation is fairly small when considering the real soil behavior and the theoretical assumptions involved in soil mechanics.

BIBLIOGRAPHY

Caquot, A., and J. Kerisel. "Sur le terme de surface dans le calcul des fondations en milieu pulverulent." Proceedings, Third International Conference on Soil Mechanics and Foundation Engineering, Vol. I. Zurich, Switzerland, 1953.

De Beer, E. E., and A. Vesic. "Etude experimentale de la capacite portante du sable sous des fondations directes etablies en surface." Annales des Travaux Publics de Belgique, Vol. 59, No. 3, 1958.

Ko, H. Y., and L. W. Davidson. "Bearing Capacity of Footings in Plane Strain." Journal of the Soil Mechanics and Foundations Division, ASCE, Vol. 99, No. SM1, Proc. Paper 9496, 1973.

Lee, K. L. "Comparison of Plane Strain and Triaxial Tests on Sand." Journal of the Soil Mechanics and Foundations Division, ASCE, Vol. 96, No. SM3, Proc. Paper 7276, 1970.

Lundgren, H., and K. Mortensen. "Determination by the Theory of Plasticity of the Bearing Capacity of Continuous Footings on Sand." Proceedings, Third International Conference on Soil Mechanics and Foundation Engineering, Vol. I. Zurich, Switzerland, 1953.

Mandel, J., and J. Salencon. "Force portante d'un sol une assise rigide." Proceedings, Seventh International Conference on Soil Mechanics and Foundation Engineering, Vol. 2. Mexico City, Mexico, 1969.

_____. "Force portante d'un sol sur une assise rigide (etude theorique)." Geotechnique, Vol. 22, No. 1, 1972.

Meyerhof, G. G. "An Investigation of the Bearing Capacity of Shallow Footings on Dry Sand." Proceedings, Second International Conference on Soil Mechanics and Foundations Engineering, Vol. 1. Rotterdam, The Netherlands, 1948.

_____. "The Ultimate Bearing Capacity of Foundations." Geotechnique, Vol. 2. London, England, 1951.

Meyerhof, G. G., and T. K. Chaplin. "The Compression and Bearing Capacity of Cohesive Layers." British Journal of Applied Physics, Vol. 4, 1953.

Meyerhof, G. G. "Ultimate bearing capacity of footings on sand layer overlying clay." Canadian Geotechnical Journal, Vol. II, No. 2, 1974.

Milovic, D. M., and J. P. Tournier. "Comportement de foundations reposant sur une couche compressible d'epaisseur limitee." Proc. Conf. u Comportement des Sols Avant La Rupture. Paris, France, 1971.

Prandtl, L. "Uber die Eindringungsfestigkeit plastisher Baustoffe und die Festigkeit von Schneiden." Zeitschrift fur Angewandtle Mathematik und Mechanik, Vol. 1, No. 1. Basel, Switzerland, 1921.

Reissner, H. "Zum Erddruckproblem." Proceedings. First International Conference on Applied Mechanics. Delft, The Netherlands, 1924.

Terzaghi, K. Theoretical Soil Mechanics. New York, N. Y.: John Wiley and Sons, Inc., 1943.

Vesic. A. S. "Analysis of ultimate loads of shallow foundations." Journal of the Soil Mechanics and Foundations Division, ASCE, Vol. 99, No. SM1, 1973.